

國立臺灣大學理學院物理學研究所



碩士論文

Department of Physics

College of Science

National Taiwan University

Master Thesis

KMY 模型中的黑洞類型

Classification Of Black Holes In KMY Model

楊書容

Shu-Jung Yang

指導教授：賀培銘 博士

Advisor: Pei-Ming Ho, Ph.D.

中華民國 108 年 8 月

Aug 2019

謝辭



首先我想向我的指導老師賀培銘教授表達最誠摯的感謝，老師總是非常溫暖和有耐心，不管我遇到什麼困難，老師都非常用心的幫助我、鼓勵我，引導我學會發問以及解答問題的能力。老師嚴謹的治學態度深深令我敬佩，是我一輩子學習的榜樣。

接著我也要感謝Yoshinori Matsuo博士在程式以及研究方向上的建議與幫忙。同時我也非常感謝協作者秦逸群，在我剛進入碩士班時常毫無頭緒時給予我非常多幫助，使我漸漸能進入狀況。也感謝黃宇廷教授、陳恆榆教授以及Takeo Inami教授啟發我對理論物理的興趣。也特別感謝黃宇廷教授和高賢忠教授願意作為我的口試委員。

當然也感謝研究室的同學們（張順晴、林宏驊、柳君諭、王塏德、蔡勝聖、鍾明志、郭家愷、李志中、郭恩瑞、周士凱、譚敏君）在研究和課業上互相幫忙，以及大學同學們（畢旅團、NI、永續部）不時的加油打氣。

最後，我最想感謝我的父母、家人和均均給予我無盡的愛、陪伴和支持，讓我得以全心全意的追求自己喜歡的事物。

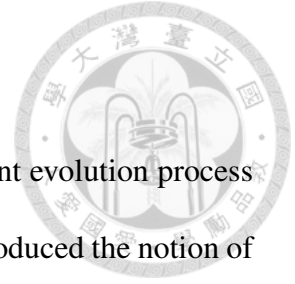
摘要



由Kawai、Matsuo及Yokokura所提出的KMY模型藉由計算半古典愛因斯坦方程得到自洽的黑洞演化，並發現此模型中之黑洞並不存在視界面（horizon）。本論文主要藉由不同初始條件探討KMY模型中所有黑洞類型的可能性，透過數值模擬以及解析表述，我們發現有兩種黑洞類型，一是在KMY模型中已被提出的漸近黑洞類型(asymptotic black hole)，另一則是類薄殼黑洞(pseudo thin shell)。若塌縮物質的初始能量密度小於某臨界值，將形成漸近黑洞，反之則形成類薄殼黑洞。

關鍵字：KMY 模型, 霍金輻射, 反饋作用, 半古典愛因斯坦方程, 漸近黑洞類型

Abstract



By solving the semi-classical Einstein equation to get a self-consistent evolution process for black holes, the earlier work of Kawai, Matsuo and Yokokura introduced the notion of a black hole where there is no horizon. In this thesis, we use both numerical simulation and analytic expression to probe the possibility of other solutions to the semi-classical Einstein equation. We find that there are two types of solutions corresponding to different initial conditions. Whenever the initial energy density of the collapsing matter is smaller than a critical value, we arrive at an asymptotic black hole. We also derive the analytic expression for the second kind of black hole. They appear when the initial energy density is higher than the critical value, and they will be called pseudo thin shells.

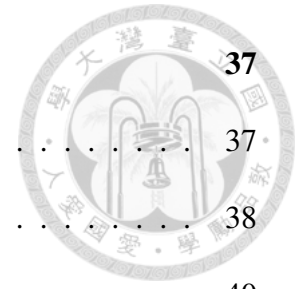
Keywords: the KMY model, Hawking radiation, back reaction, semi-classical Einstein equation, asymptotic black hole states



Contents

1	Introduction	5
2	The Conventional Model Of Black Hole	9
2.1	Schwarzschild Metric	9
2.2	Hawking Radiation	10
2.3	Information Loss Paradox	13
3	The KMY Model	14
3.1	No Horizon In The KMY Model	20
3.2	Implication Of The KMY Model On Information Loss Paradox	21
4	Unphysicalness Of Ideal Thin Shell	22
4.1	Ideal Thin Shell	23
4.1.1	Constant Schwarzschild Radius	24
4.1.2	Shrinking Schwarzschild Radius	25
4.2	Pseudo-Thin Shell	26
4.3	Make Sense Of Thin Shells	30
5	The First Asymptotic States: Slope-1 Shell	33
5.1	Purpose Of Numerical Simulation	36

6	Numerical Simulation Setup	37
6.1	Each Discrete Shell As Pseudo-thin Shell	37
6.2	Removing Higher Derivatives	38
6.3	How To Interpret The Profile	40
6.4	Massive Core Inside The Collapsing Shells	42
7	Asymptotic States	44
7.1	a-r Graph In Static Background	44
7.2	a-r Graph in the KMY Model	47
7.3	Details Of The Profiles	52
7.4	Small Slope	52
7.5	Large Slope	55
8	Stability Of The Decaying Rate	58
9	Discussion and Conclusion	63
	Bibliography	65
	Appendix	69





List of Figures

2.1	At the late stage of the collapsing process Hawking radiation should arise	12
4.1	The evaporation of an ideal thin shell terminates	26
7.1	$a-r$ graph for $\partial a/\partial r = 0.00001, 1, 1.1, \infty$	46
7.2	$a-r$ graph for $\frac{\partial a}{\partial r} = \infty$	49
7.3	$a-r$ graph for $\frac{\partial a}{\partial r} = 10$	49
7.4	$a-r$ graph for $\frac{\partial a}{\partial r} = 0.1$	50
7.5	$a-r$ graph for $\frac{\partial a}{\partial r} = 1$	50
7.6	$a(u)$ for $da/dr = 0.1$	53
7.7	$a(u)$ for $da/dr = 1$	54
7.8	$m(u)$ for $\partial a/\partial r = 0.1$	54
7.9	$m(u)$ for $\partial a/\partial r = 1$	55
7.10	$a(u)$ for $\partial a/\partial r = \infty$	56
7.11	$a(u)$ for $\partial a/\partial r = 10$	56
7.12	$m(u)$ for $\partial a/\partial r = \infty$	57
7.13	$m(u)$ for $\partial a/\partial r = 10$	57
8.1	The first order correction in Hawking radiation for $\frac{da}{dr} = 0.1$	59
8.2	The first order correction in Hawking radiation for $\frac{da}{dr} = 1$	60

8.3	The first order correction in Hawking radiation for $\frac{da}{dr} = \infty$	61
8.4	The first order correction in Hawking radiation for $\frac{da}{dr} = 10$	62





Chapter 1

Introduction

In the study of the black holes, it is common practice to study the formation and evaporation of a black hole separately as independent processes for the simplicity of calculation. During the formation process, which is typically treated as a purely classical process, classical matter collapses and an event horizon appears. After that, the evaporation process due to quantum effect is considered as an independent process. In this approximation scheme, the evaporation is computed in the presence of the event horizon of a classical black hole with a constant Schwarzschild radius.

Of course, in reality, the Schwarzschild radius must decrease over time if the black hole completely evaporates in the end. But some people argued that the extremely slow change in the Schwarzschild radius can be ignored for the study of the black-hole evaporation. As a test of the robustness of these arguments, one should check whether the evaporation is significantly modified if the time-dependence of the Schwarzschild radius is turned on. Generically, when the collapsing matter is very close to its Schwarzschild radius, Hawking radiation is supposed to arise because the spacetime structure has been significantly changed, and hence the vacuum state defined in the infinite past will contain

particles after sufficient collapsing time.

In the work done by Kawai, Matsuo, and Yokokura [1], they describe the evolution of a black hole by viewing the formation and the evaporation as a single and continuous process. They include the back reaction from Hawking radiation at the very beginning of the formation process of a black hole. The Schwarzschild radius is time-dependent due to Hawking radiation. We will refer to the approach of Ref. [1], which is followed by Refs. [2]–[6], as the KMY model.

They found that there are two distinct types of solutions. The first type is by considering the collapse of an ideal thin shell, i.e. a shell with zero thickness or delta function energy distribution. It will not evaporate totally and approaches a classical black hole in the infinite future with an event horizon. On the other hand, if the collapsing matter has a smooth density distribution, without even specified the initial density of the distribution, it will always evaporate totally without apparent horizon. Recall that in 2d black hole we also have seen similar categorization of black holes. In [8], it is shown that an apparent horizon will either appear or not depends on the energy flux distribution, resulting in also two types of black holes.

Given the distinct behaviors of these two types of distribution, several interesting questions arise. For example, is the ideal thin shell of delta-function energy distribution physical? Are there other classes of behaviors characteristically different from the two classes of solutions already found in Ref. [1]?

In this paper, we first discuss the difference between the thin shell with delta function energy distribution and that with finite but very small thickness. These two shells should be almost indistinguishable if the finite thickness is very close to (but still larger than) the cut-off scale of the theory. However, they have characteristically different behaviors

in calculations of the Hawking radiation. We shall demonstrate the difference by comparing a thin shell with thickness of Planck scale and a shell with a delta function energy distribution. While the latter survives in the end as a classical black hole, the former evaporates completely within finite time. Thus, the thin shell with delta function thickness is unphysical, and hence we will focus on the configurations with finite thickness of Planck scale.

Secondly, we will show that there are at least two classes of asymptotic behaviors of the collapsing matter as a result of the back reaction of Hawking radiation. Besides the asymptotic state found in Ref. [1], which will be called *slope-1 shell* in the following, the other class is described as a thin shell in the low-energy theory, but it should not be identified with the ideal thin shell of zero thickness. We will examine the details of both classes of collapsing processes in this paper through both analytical study and numerical simulations.

The plan for this thesis is the following. In chap.2, we will review the conventional model for black hole formation and evaporation, with an emphasis on the nature of Hawking radiation generated in the collapsing process. In chap.3, we will review the KMY model and comment on how the absence of horizon implicate the possible resolution to information loss paradox. In chap.4 we will review the behavior of first type of solution already proposed in the KMY model, the ideal thin shell, but contrasts it with a pseudo-thin shell to show the unphysicalness of an ideal thin shell. In chap.5, we will review the other type of solution, the slope-1 asymptotic state. We will then discover another asymptotic state, the pseudo-thin shell, by numerical simulation in chap.7 after introducing the setup for numerical simulation in chap.6. We will also compare the details about the profiles of the collapsing shells in both static and time-dependent background in chap.7. Finally, we

summarize the finding of this work in chap.9.





Chapter 2

The Conventional Model Of Black Hole

In this chapter, we will briefly review the conventional model of black hole and point out the main issues in this model.

2.1 Schwarzschild Metric

In the formation of a black hole, one usually considers the gravitational collapse of a matter shell ultimately falls into its Schwarzschild radius and an event horizon forms. The spacetime outside the collapsing shell can be represented by the well-known Schwarzschild metric,

$$ds^2 = -\left(1 - \frac{a}{r}\right)dt^2 + \left(1 - \frac{a}{r}\right)^{-1}dr^2 + r^2d\Omega^2, \quad (2.1)$$

where r is the areal radius. It can also be written in terms of Eddington retarded coordinate u ,

$$ds^2 = -\left(1 - \frac{a}{r}\right)du^2 - 2dudr + r^2d\Omega^2, \quad (2.2)$$

where

$$u = t - r^* = t - \left(r + a \ln \left| \frac{r}{a} - 1 \right| \right). \quad (2.3)$$

Whereas the metric inside the shell is always the flat metric,

$$ds^2 = -dU^2 - 2dUdr + r^2 d\Omega^2, \quad (2.4)$$

where $U = t - r$.

2.2 Hawking Radiation

Then we first review the basic derivation of Hawking radiation. Please refer to the concise introduction to Hawking's original ideas in Ref. [7] for more details.

In discussing the production of Hawking radiation in the collapsing process, one usually imagines the evolution of spacetime can be divided into three phases. The first phase will be the usual Minkowski spacetime before the shells collapse. The second phase would be the collapsing process of a black hole followed by the third phase with a black hole formed and described by the Schwarzschild metric. Consider scalar field propagating through out the spacetime. The field can be decomposed into positive and negative frequency modes with respect to the killing vector in the first and third stationary spacetime. In general, the state starts as a vacuum state in the first phase will evolve into some other state with particles because the definitions of vacuum are different in these two phases. The way we get the particle numbers are by considering Bogoliubov transformation and read off the particle numbers by the Bogoliubov coefficient. The idea is straightforward but the most crucial step is to use the backward ray chasing techniques, to find the proper relation between U and u so that one can connect the field propagating from the past infinity towards the origin and reflect to go to the future infinity.

The crucial point is that whenever the Eddington retarded time U and u , inside and



outside the collapsing matter is related in an exponential manner,

$$U = U_0 - Ae^{-ku}, \quad (2.5)$$



for some constant U_0 , A and k , we will get a Hawking-like particle spectrum,

$$\frac{1}{e^{2\pi\omega/k} - 1}, \quad (2.6)$$

where Hawking temperature is $T = k/2\pi$.

The calculation of Hawking radiation can be carried out in another brilliant way. In Ref. [23] a model of moving mirror is proposed to get a better understanding of the production of Hawking radiation. It will then be used in Ref. [24] for the calculation of Hawking radiation, and then widely used in the literature. Following these works, also approximating the vacuum energy-momentum tensor by that of s-wave modes of massless scalar fields, and assuming that the initial state in the infinite past is the Minkowskian vacuum state, the Hawking radiation is given by the energy flux

$$T_{uu} = \frac{\mathcal{N}}{4\pi r^2} \{u, U(u)\}, \quad (2.7)$$

where $\kappa = 8\pi G$, \mathcal{N} is a numerical constant proportional to the number of massless fields in Hawking radiation and $\{u, U(u)\}$ is the Schwarzian derivative defined by

$$\{u, U(u)\} \equiv \left[\frac{\frac{d^2 U(u)}{du^2}}{\frac{dU(u)}{du}} \right]^2 - \frac{2}{3} \frac{\frac{d^3 U(u)}{du^3}}{\frac{dU(u)}{du}}. \quad (2.8)$$

Note that in the conventional collapsing model above, there will be a negative energy flow across the horizon to compensate for the positive energy flow to the future infinity

by the conservation of energy momentum tensor.

An intuitive picture is to consider particle creation around the event horizon with particle escape to infinity and anti-particle flow into the horizon.

There are two main issues in this conventional model for the formation and the evaporation of a black hole. The first one is that at the late stage of the collapse, the shells have already been very close to their Schwarzschild radius. In fact, we cannot distinguish this configuration from the already formed black hole, or, classical black hole, because both have a very large redshift near the surface of the horizon viewed from a distant observer.

In particular, from the explanation above, we know that whenever the redshift is large in an exponential manner, Hawking radiation should arise. Therefore, at the late stage of collapse, we should not ignore the effect of Hawking radiation but should incorporate them by semi-classical approach. This concern is pictured in the fig. 2.1 below.

The second issue in the conventional model is the information loss paradox described below.

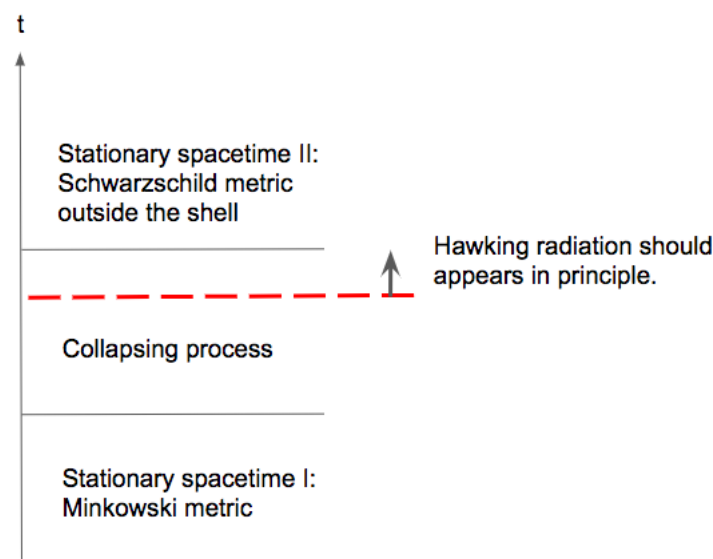


Figure 2.1: At the late stage of the collapsing process Hawking radiation should arise

2.3 Information Loss Paradox



Here we briefly review the issues in the information loss paradox. This is based on the discussion in Ref. [9].

The conventional model of black hole formation and evaporation will give rise to the information loss paradox. In this paradox, the presence of an event horizon is critical to the phenomenon, because once the collapsing matter falls into the event horizon, we can only count on Hawking radiation to transfer all the information to the future infinity before the black hole evaporates totally. If not, after total evaporation, all the information that falls into the event horizon would disappear.

The first issue is that Hawking radiation cannot carry out all the information to the future infinity, as has been proven in Ref. [9] that if we assume the vacuum state deviate slightly from that in flat space around event horizon, or, in Mathur's words that the nice-ness condition is satisfied, Hawking radiation can contain only partial information about the collapsing matter.

The second issue is that if we assume the black hole can be formed by a pure state, with the total evaporation of black hole, we are left with a mixed state. The reason is that Hawking radiation would have entanglement with matter inside the black hole. One might want to oppose the second issue by considering a black hole remnant containing the entanglement entropy with the outside Hawking radiation. However, this way, there should be a lower bound on the entanglement entropy for this remnant which, with only finite amount of size, should not naturally satisfy this lower bound.

This way, although Hawking radiation might appear thermal, by appearing as a Planck distribution, it has very different nature from ordinary thermal waves.



Chapter 3

The KMY Model

In this chapter, we review the main results of the KMY model. A crucial point of the KMY model is that the back reaction of Hawking radiation to the geometry is not ignored as it was in many other papers, but fully implemented through the semi-classical Einstein equation. First, they consider two assumptions: (1) spherical symmetric, (2) hawking radiation is composed of massless scalar traveling at the speed of light. They first study the collapsing process of a single shell, and then generalize it to the continuous shell case.

In the single shell case, they construct the model by combining the flat metric inside the shell and outgoing vaidya metric outside the shell. That is, the metric inside the shell satisfy the vacuum solution of Einstein equation for there is no matter inside. we can use the flat metric,

$$ds^2 = -dU^2 - 2dUdr + r^2d\Omega^2, \quad (3.1)$$

where U is the time coordinate inside the shell, and r is the radius of 2-sphere.

On the other side of the shell, It is assumed that there is only outgoing massless dust emitting around the shell. That is, we assume the vacuum energy momentum tensor is dominated by outgoing Hawking radiation. This means that at both spacetime around

the collapsing shell and spatial infinity we have only outgoing Hawking radiation. The Hawking radiation is created during the gravitational collapse because the quantum vacuum state of incoming matter in the infinite past evolves to a state that is no longer the vacuum state at large r after the gravitational collapse.

Note that the situation is different in the conventional model. In conventional model, the outgoing flux is zero at the horizon whereas there is negative energy ingoing into the horizon, which is compensated by the outgoing positive energy flow at the spatial infinity.

Therefore we can use the outgoing vaidya metric as the most general form to describe the spacetime outside the shell, ie.

$$ds^2 = -\left(1 - \frac{a(u)}{r}\right)du^2 - 2dudr + r^2d\Omega^2, \quad (3.2)$$

where u is the Eddington retarded time coordinate. We will use R to label the locus of the shell. Because we assume the shell is collapsing at the speed of light, the equation of motion for R is obtained on both side by setting $ds^2 = 0$, which is,

$$dR = -\frac{dU}{2}. \quad (3.3)$$

Also, from metric outside we have

$$\frac{dR}{du} = -\frac{1}{2}\left(1 - \frac{a(u)}{r}\right). \quad (3.4)$$

From this, we can relate U and u as,

$$dU = \left(1 - \frac{a(u)}{r}\right)du. \quad (3.5)$$

The only non-vanishing component of $G_{\mu\nu}$ for outgoing vaidya metric is

$$G_{uu} = -\frac{\dot{a}}{r^2}. \quad (3.6)$$

Therefore, from the semi-classical Einstein equation,

$$G_{\mu\nu} = 8\pi G \langle T_{\mu\nu} \rangle, \quad (3.7)$$

we can obtain \dot{a} by calculating $\langle T_{\mu\nu} \rangle$. Here, $\langle T_{\mu\nu} \rangle$ is obtained by calculating the difference of the vacuum expectation value of energy momentum tensor inside and outside the shell.

The equation for a is obtained as

$$\frac{da}{du} = \frac{-\hbar G}{4\pi} \{u, U\} = \frac{-\hbar G}{4\pi} \left(\frac{\ddot{U}^2}{\dot{U}^2} - \frac{2\ddot{U}}{3\dot{U}} \right), \quad (3.8)$$

where \dot{U} is $\frac{dU}{du}$ and $\{u, U\}$ is the Schwarzschild derivative. Therefore we obtain the equations for both $a(u)$ and $R(u)$. The main result from solving the equations is that a single shell will not always evaporate totally unless the initial mass is very small.

The single shell model can be generalized to a continuous shell model. Let the collapsing matter be divided into infinitely many shells. We will label the shell from outside. For example, the radius of the outermost shell is labeled by R_0 , and its Schwarzschild radius is denoted as a_0 . The Eddington retarded time coordinate outside and inside R_0 is defined as u_0 and u_1 respectively. By analogy, the equation for R_α in its own time coordinate is simply

$$\frac{dR_\alpha}{du_\alpha} = -\frac{1}{2} \left(1 - \frac{a_\alpha(u_\alpha)}{R_\alpha(u_\alpha)} \right). \quad (3.9)$$

And the equation for a_α is

$$\frac{da_\alpha}{du_\alpha} = -\frac{N_0 l_p^2}{48\pi} \{u_\alpha, U\}, \quad (3.10)$$

where l_p is $\sqrt{\hbar G}$, and N_0 is the number of species of massless free scalar, u_α is the time coordinate for each shell label by α , and U is the time coordinate for the innermost shell.

With the continuity condition, we can relate the time coordinate u_α and $u_{\alpha-1}$ on both sides of the shell with radius R_α as

$$\frac{du_{\alpha+1}}{du_\alpha} = \frac{R_\alpha - a_\alpha}{R_\alpha - a_{\alpha+1}}. \quad (3.11)$$

And also the energy flux between the $\alpha - 1^{th}$ and the α^{th} layer of the shell is

$$J_\alpha = \frac{\hbar}{8\pi} \{u_\alpha, u_{\alpha+1}\}. \quad (3.12)$$

With the identity of Schwarzschild derivative,

$$\{u_\alpha, U\} = \{u_{\alpha+1}, U\} \left(\frac{du_{\alpha+1}}{du_\alpha} \right)^2 + \{u_\alpha, u_{\alpha+1}\} \quad (3.13)$$

We can also express eq. (3.10) equivalently as,

$$\frac{da_\alpha}{du_\alpha} = \frac{da_{\alpha+1}}{du_{\alpha+1}} \left(\frac{du_{\alpha+1}}{du_\alpha} \right)^2 + \{u_\alpha, u_{\alpha+1}\} \quad (3.14)$$

We can define

$$e^{\psi_\alpha(u_\alpha(u))} \equiv \frac{du_\alpha(u)}{du_0} \equiv \frac{du_\alpha(u)}{du}. \quad (3.15)$$

It can then promote α as a continuous parameter by defining $\psi(u, r) = \psi_\alpha(u_\alpha(u))$ and $a(u, r) = a_\alpha(u_\alpha(u))$. Please refer to Ref. [6] for further details about the generalization.

Also, the metric just outside the α^{th} shell, that is R_α can be written as,

$$ds^2 = -\left(1 - \frac{a_\alpha(u_\alpha)}{r}\right)du_\alpha^2 - 2du_\alpha dr + r^2 d\Omega^2, \quad (3.16)$$



which is equivalent to,

$$ds^2 = -e^{2\psi(u,r)} \left(1 - \frac{a(u,r)}{r}\right) du^2 - 2e^{\psi(u,r)} du dr + r^2 d\Omega^2. \quad (3.17)$$

The time evolution of this metric will be studied in terms of the Eddington retarded time u . Due to spherical symmetry, the functions $\psi(u, r)$ and $a(u, r)$ only depend on u and the areal radius r .

At any given instant of time u , the function $a(u, r)$ in the metric (3.17) gives twice the Bondi mass inside the ball of radius r centered at the origin. The other function $\psi(u, r)$ in the metric (3.17) is the exponent of the red-shift factor $e^{\psi(u,r)}$ between the retarded time coordinate u at spatial infinity and the retarded time coordinate $\hat{u}(u, r)$ at r [6].

This metric is only applicable to the region of space-time outside the event horizon if it exists. Whether there is an event horizon should be determined by the time evolution of a given initial state. In principle, one can use this metric until a singularity appears to mark the location of the event horizon.

We assume that the collapsing matter has an outer radius $R_0(u)$ beyond which there is no ingoing energy flux (but there can be outgoing energy flux as Hawking radiation) so that $a(u, r)$ is r -independent outside the outer radius $R_0(u)$:

$$a(u, r) = a_0(u) \quad \text{for} \quad r \geq R_0(u) \quad (3.18)$$

for some function $a_0(u)$ which is twice the total Bondi mass of the collapsing matter.

When $a_0(u)$ is time-independent, as in the classical case without Hawking radiation, the metric (3.17) is equivalent to the Schwarzschild metric with Schwarzschild radius a_0 for $r > R_0(u)$. When $a_0(u)$ is not time-independent, there is an outgoing energy flux for $r > R_0(u)$ given by

$$T_{uu} = -\frac{1}{8\pi Gr^2} \frac{da_0(u)}{du}. \quad (3.19)$$

For simplicity, in this paper, we shall assume that the collapsing matter is falling at the speed of light. Applying the general results of Ref. [6] to this special case, the red-shift factor $e^{\psi(u,r)}$ is given by

$$\psi(u, r) = -\int_r^\infty d\bar{r} \frac{\frac{\partial a(u, \bar{r})}{\partial \bar{r}}}{\bar{r} - a(u, \bar{r})}. \quad (3.20)$$

Because of eq.(3.18), $\psi(u, r) = 0$ for $r > R_0(u)$.

According to eq.(3.20), the red-shift factor for the retarded time U of the Minkowski space inside the collapsing matter is

$$\log \left(\frac{dU(u)}{du} \right) = \psi_0(u) = -\int_0^{R_0(u)} dr \frac{\frac{\partial a(u, r)}{\partial r}}{r - a(u, r)}. \quad (3.21)$$

Since only the regions with $\frac{\partial a(u, r)}{\partial r}$ contribute to the integral above and $a(u, r)$ is always a monotonic function of r , u and a can be treated as coordinates to parametrize these regions. Then, r is a function of u and a , and the integral (3.21) can also be expressed as

$$\psi_0(u) = -\int_0^{a_0(u)} \frac{da}{r(u, a) - a}. \quad (3.22)$$

Using eq.(3.21), one can rewrite the Schwarzian derivative as

$$\{u, U(u)\} \equiv \frac{1}{3} [\psi_0^2(u) - 2\ddot{\psi}_0(u)], \quad (3.23)$$



where the dots denote u -derivatives.

3.1 No Horizon In The KMY Model

It was shown in Ref. [1] that there would no event or apparent horizon for a certain smooth configuration, which was called “asymptotic black holes” in Ref. [6], and it will be referred to as the “slope-1” configuration.

It was proven later in Refs. [3, 5] that there is no apparent horizon as long as the collapsing matter completely evaporates within finite time.

According to the semi-classical Einstein equation, the Schwarzschild radius shrinks with time in a superluminal fashion due to the loss of energy into Hawking radiation. As a result, the collapsing matter can never fall through the Schwarzschild radius, as long as the (incipient) black hole evaporates completely within finite time [1, 3].

To be more specific, as mentioned in Ref. [3], consider the radial trajectory $r(u) = a(u) + \eta$ of a point just outside the Schwarzschild radius, where η is a very small positive constant. Then the collapsing speed of the point, $\dot{r}(u)$, where the dot means derivative with respect to u , can be approximated by the decaying rate of the Schwarzschild radius, $\dot{a}(u)$, and we have

$$ds^2 \simeq \left(-\frac{\eta}{a(u)} - 2\frac{da(u)}{du} \right) du^2. \quad (3.24)$$

We then see that as long as η is smaller than $-2a(u)\dot{a}(u)$, the trajectory would be space-like. This means that there is a barrier that the collapsing shells can never cross as long as

$$\dot{a}(u) < 0.$$

The possibility that the back reaction of Hawking radiation in the near horizon region can be so large as to remove the horizon has also been proposed by many others [10]–[22].



3.2 Implication Of The KMY Model On Information Loss Paradox

This section is based on Ref. [3] and Ref. [6]. As we mentioned in Chap.2.3, Hawking radiation cannot carry out all the information of the collapsing matter falling inside the event horizon before the black hole evaporates totally. But the entanglements between them imply that after the total evaporation we are left with a mixed state whereas we start from a pure state.

However, in the KMY model, there is nor event horizon or apparent horizon. Therefore, at least we do not have the mixed state problem, because the collapsing matter can never catch up with its Schwarzschild radius and everything stays outside the event horizon. On the other hand, how can we ensure that Hawking radiation indeed carries out all the information of the collapsing shells?

From Ref. [6] we can get some intuition by calculating the energy momentum tensor in the tangential direction and that of the collapsing matters. We find that both are at Planck scale. With this high energy scale, we could only trust a consistent theory for quantum gravity which should by itself be unitary. Therefore, we neither need to worry about information loss in this case.



Chapter 4

Unphysicalness Of Ideal Thin Shell

In this chapter, we first review the case of an ideal thin shell, i.e. a thin shell of zero thickness. Then we compare it with the notion of a pseudo-thin shell, which has a thickness larger than the Planck length. Their behaviors turn out to be characteristically different.

It was shown in Ref. [1] that an ideal thin shell does not necessarily evaporate completely, depending on the initial condition. Its Hawking radiation decreases with time so fast that the total outgoing energy is still much less than the mass of the black hole even in the infinite future and an event horizon arises like a classical black hole [1].

However, it is not natural to find a shell with delta-function-like energy distribution in nature. Even if we are dealing with very dense distribution, we can always divide the mass into infinitely many shells within a narrow region. Therefore, it is more appropriate to consider a continuous distribution of mass with many layers of shells.

Also, it is important to note the time evolution of a thin shell of absolutely zero thickness may or may not be the continuous limit of a thin shell of finite thickness, as the equation determining Hawking radiation involves second order derivatives.

We carefully investigate in this paper whether small deviations from the perfect math-

ematical notion of the zero-thickness thin shell would lead to characteristically different space-time structures at large scales.



4.1 Ideal Thin Shell

For a thin shell of zero thickness, we have

$$a(u, r) = a_0(u) \Theta(r - R_0(u)), \quad (4.1)$$

where $\Theta(x)$ is the step function that is 0 or 1 for $x < 0$ or $x > 0$. It has a diverging energy density proportional to the Dirac delta function that diverges at $r = R_0(u)$. While a physical shell must have a finite thickness much larger than the Planck length, and an energy density much smaller than the Planck scale to justify the use of low-energy effective theories, this notion of an ideal thin shell has been widely used in the literature.

To evaluate $\psi_0(u)$, we use (3.22), an integral with respect to a . The inverse function of the step function (4.1) gives a constant function with respect to a ,

$$r(u, a) = R_0(u) . \quad (4.2)$$

The integral (3.22) is expressed as

$$\psi_0(u) = - \int_0^{a_0(u)} \frac{da}{R_0(u) - a}, \quad (4.3)$$

and we find

$$\psi_0(u) = \log \left(\frac{R_0(u) - a_0(u)}{R_0(u)} \right). \quad (4.4)$$



4.1.1 Constant Schwarzschild Radius

Let us first consider the evolution of the ideal thin shell in the fixed Schwarzschild background, ignoring the back reaction of Hawking radiation.

The thin shell is by assumption falling at the speed of light, hence we have

$$\frac{dR_0(u)}{du} = -\frac{1}{2} \frac{R_0(u) - a_0(u)}{R_0(u)} \quad (4.5)$$

according to the metric (3.17). When a_0 is assumed to be time-independent, its solution is

$$R_0(u) \simeq a_0 + C_0 e^{-\frac{u}{2a_0}} \quad (4.6)$$

when $R_0(u) - a_0 \ll a_0$. Eq.(4.4) then gives

$$\psi_0(u) \simeq -\frac{1}{2a_0} + \text{const.}, \quad (4.7)$$

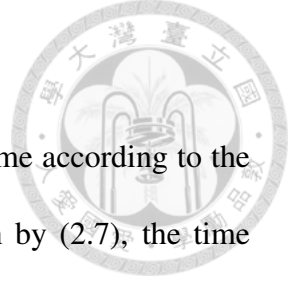
and the Schwarzian derivative can be easily computed

$$\{u, U(u)\} = \frac{1}{3} (\dot{\psi}_0^2 - 2\ddot{\psi}_0) \simeq \frac{1}{12a_0^2}, \quad (4.8)$$

which gives the conventional result of Hawking radiation

$$\frac{da_0}{du} \simeq -\frac{N_0 l_p^2}{48\pi a_0^2}. \quad (4.9)$$

As a result, the thin shell evaporates completely within finite time $\propto a_0^3$.



4.1.2 Shrinking Schwarzschild Radius

However, as there is Hawking radiation, $a_0(u)$ must decrease over time according to the outgoing energy flux (3.19). Since the Hawking radiation is given by (2.7), the time evolution of $a_0(u)$ is given by the differential equation;

$$\frac{da_0(u)}{du} = \frac{-N_0 l_p^2}{4\pi} \{u, U\}. \quad (4.10)$$

This modification would change the evaluation of $\psi_0(u)$ (4.7). Using eqs.(4.4) and (4.5), we find

$$\psi_0(u) \simeq -\frac{a_0(u)}{2R_0^2(u)} - \frac{\dot{a}_0(u)}{R_0(u) - a_0(u)}. \quad (4.11)$$

While the first term is always finite, the 2nd term diverges at the horizon unless $\dot{a}_0(u)$ vanishes at the horizon. Given eq.(2.7) and eq.(3.23), it is inconsistent to have a diverging ψ_0 at the horizon, hence \dot{a}_0 must vanish at the horizon. The conclusion is thus that once the time-dependence of the Schwarzschild radius $a(u)$ is taken into account, the ideal thin shell cannot cross the horizon without turning off Hawking radiation. Indeed, it was shown in Ref. [1] that the Hawking radiation decreases to zero and a classical black hole survives the incomplete evaporation for a collapsing ideal thin shell.

More explicitly, assuming that change of $a_0(u)$ is very slow, eq.(4.5) implies that the shell asymptotes to the Schwarzschild radius $r = a_0(u)$. When the shell has approached the Schwarzschild radius sufficiently, the radius on the shell would be approximated by the Schwarzschild radius, $R_0(u) \simeq a_0(u)$. Then, (4.10) is solved with

$$u = \frac{e^{-\frac{D^2}{2}}}{6\pi B} \int_D^\xi d\xi' e^{\frac{\xi'^2}{4}}, \quad (4.12)$$

$$a(u) = a(0) - B \int_D^\xi d\xi' e^{-\frac{\xi'^2}{4}} \quad (4.13)$$

for constant parameters B, D . This solution describes a decaying Hawking radiation that vanishes at the event horizon and the ideal thin shell is not completely evaporated. See Fig.4.1 for the numerical simulation.

To summarize, for the ideal thin shell, if we ignore the time-dependence of the Schwarzschild radius, the black hole would completely evaporate as in the conventional model; but if we account for the time dependence of the Schwarzschild radius, the black hole would not evaporate completely. While one may suspect that certain omitted details of the quantum effect involved in this process could further change the conclusion, it is, to say the least, an example showing that the back reaction of Hawking radiation has the potential to play a crucial role. Calculations without back reaction needs to be further justified.

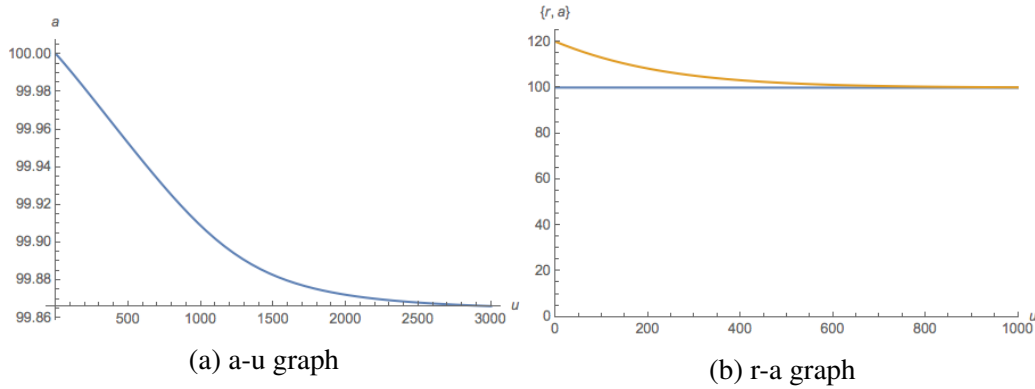
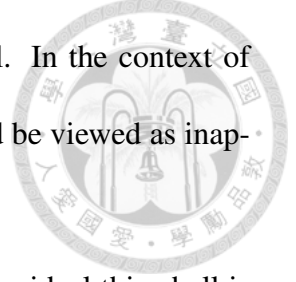


Figure 4.1: The evaporation of an ideal thin shell terminates

4.2 Pseudo-Thin Shell

Here we discuss the notion of a “pseudo thin shell”, which is a configuration indistinguishable from the ideal thin shell in a low-energy effective theory with a cutoff length scale ℓ much larger than the Planck length ℓ_p . However, it turns out that the behavior of the pseudo thin shell is characteristically different from the ideal thin shell (when the time-dependence of the background is turned on). This means that we cannot trust the

low-energy effective theory on its description of the ideal thin shell. In the context of low-energy effective theories, the notion of the ideal thin shell should be viewed as inapplicable.



The purpose of this subsection is only to point out the fact that the ideal thin shell is over-sensitive to details at the Planck scale. For this purpose, we do not have to justify our choice of the profile for the pseudo thin shell. Nevertheless, the pseudo thin shell is clearly a natural consideration as an interpolation between the ideal thin shell and the slope-1 configuration described in the next section. We will have more discussions on the pseudo thin shell in the next subsection.

Here, we consider the pseudo thin shell with the following profile;

$$a(u, r) \simeq \left(r - \frac{2\sigma}{r} \right) [\Theta(r - R_i(u)) - \Theta(r - R_0(u))] + a_0(u)\Theta(r - R_0(u)), \quad (4.14)$$

where R_0 and R_i are the outer and inner radii, and $R_0(u) - R_i(u)$ is assumed to be much smaller than $R_0(u)$. This pseudo thin shell still contains an ideal thin shell at the innermost surface. While this does not interfere with our purpose to show that a small deviation from an ideal thin shell makes a large difference, the difference between an ideal thin shell only at the inner most surface and a finite-density distribution everywhere is negligible since physics at the innermost part is almost irrelevant due to the large red shift factor as we will see soon.

The Schwarzschild radii at the outer and inner surfaces of the shell are thus

$$a_0(u) \equiv R_0(u) - \frac{2\sigma}{R_0(u)}, \quad (4.15)$$

$$a_i(u) \equiv R_i(u) - \frac{2\sigma}{R_i(u)}. \quad (4.16)$$

These formulas, together with the assumption that the shells are collapsing at the speed of light, imply that the Schwarzschild radii $a(u)$ changes with time according to the conventional formula of Hawking radiation $\dot{a} \simeq -\sigma/a^2$ for some constant σ . In comparison with eq.(4.9), σ is a constant parameter of Planck scale

$$\sigma \simeq \frac{\kappa \mathcal{N}}{48\pi} \sim \mathcal{O}(\ell_P^2), \quad (4.17)$$

where \mathcal{N} was defined in eq.(2.7). We shall compare the rates of evaporation for a pseudo thin shell and an ideal thin shell, taking into consideration the time-dependence of the Schwarzschild radius.

Within the shell ($r \in (R_i(u), R_0(u))$), this is the same profile as the asymptotic black holes proposed in Ref. [1] (to be discussed below in Chap.5). But at a length scale much larger than the thickness $\Delta R \equiv R_0(u) - R_i(u)$, its profile is essentially the same as that of the ideal thin shell discussed above in Chap.4.1.

For this configuration (4.14), we have

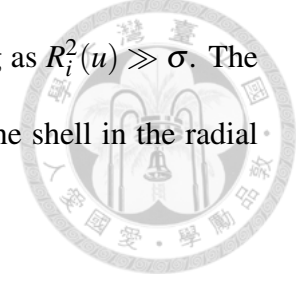
$$\begin{aligned} \psi_0(u) &\simeq \log \left(\frac{R_i(u) - a_i(u)}{R_i(u)} \right) - \frac{R_0^2(u) - R_i^2(u)}{2\sigma} \\ &\simeq \log \left(\frac{\sigma}{R_i^2(u)} \right) - \frac{R_0^2(u) - R_i^2(u)}{2\sigma} \\ &\simeq -\frac{R_0^2(u) - R_i^2(u)}{2\sigma}, \end{aligned} \quad (4.18)$$

where in the last line we have assumed that

$$\Delta R(u) \equiv R_0(u) - R_i(u) \gg \frac{\sigma}{R_i(u)} \log \left(\frac{R_i^2(u)}{\sigma} \right). \quad (4.19)$$

Notice that, since σ is of order Planck length squared, the inequality above is satisfied

even when $\Delta R \equiv R_0(u) - R_i(u)$ is as short as a Planck length as long as $R_i^2(u) \gg \sigma$. The difference in the areal radius $\Delta R(u)$ corresponds to a thickness of the shell in the radial direction of the length



$$\Delta L \equiv \sqrt{g_{rr}(R_0(u))} \Delta R(u) \gg \mathcal{O} \left(\ell_P \log \left(\frac{R_0(u)}{\ell_P} \right) \right). \quad (4.20)$$

Even for a shell as heavy as 10^{10} solar mass, ΔL only needs to be greater than 110 times the Planck length to justify the approximation above. It should be hard to distinguish a thin shell of thickness 0 or ΔL if the low-energy effective theory is not valid up to the energy scale of 10^{17} GeV.

To calculate Hawking radiation, we take the derivative of eq.(4.18):

$$\dot{\psi}_0(u) \simeq - \frac{R_0(u)\dot{R}_0(u) - R_i(u)\dot{R}_i(u)}{\sigma}. \quad (4.21)$$

As $R_i(u)$ is falling at the speed of light,

$$\begin{aligned} \frac{dR_i(u)}{du} &= -\frac{1}{2} e^{\psi(u, R_i(u))} \frac{R_i(u) - a_i(u)}{R_i(u)} \\ &\simeq -\frac{1}{2} e^{-\frac{R_0^2(u) - R_i^2(u)}{2\sigma}} \frac{R_i(u) - a_i(u)}{R_i(u)}. \end{aligned} \quad (4.22)$$

The huge red-shift factor above

$$e^{-\frac{R_0^2(u) - R_i^2(u)}{2\sigma}} \simeq e^{-\frac{R_0(u)(R_0(u) - R_i(u))}{\sigma}} \ll \frac{\sigma}{R_i^2(u)} \quad (4.23)$$

implies that the 2nd term in eq.(4.21) is much smaller than the 1st term, hence

$$\psi_0(u) \simeq -\frac{R_0(u)\dot{R}_0(u)}{\sigma} \simeq \frac{1}{2a_0(u)}, \quad (4.24)$$



which is the same as eq.(5.9) for a slope-1 shell in Chap.5, but differs from the ideal thin shell in Chap.4.1.¹ As a result, this thin shell of finite thickness will evaporate completely, like the conventional model of black holes, rather than approaching a classical black hole like the ideal thin shell.

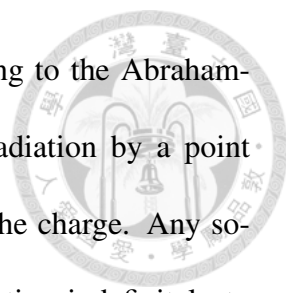
It is an amusing coincidence that the Hawking radiation of the pseudo-thin shell (with its back reaction included in the calculation) happen to agree with that of the ideal thin shell when the back reaction is ignored but disagrees with the ideal thin shell when the back reaction is turned on. Despite its sensitivity to modifications at the length scale of $100\ell_P$, this observation suggests that there might still be some robustness in the Hawking radiation of the conventional model of black holes.

4.3 Make Sense Of Thin Shells

The implication of the pseudo thin shells considered above is that the equations governing the Hawking radiation (2.7) is too sensitive to Planck-scale details so that the notion of ideal thin shells is inappropriate for discussions in the context of low-energy effective theories.

Similar issues have been discussed in other branches of physics. It is not uncommon for low-energy effective theories to involve higher-derivative terms. Typically, such higher-derivative terms lead to various pathologies. A well known simple example can be

¹ Eq.(4.24) differs significantly from the ideal thin shell which has $\dot{\psi}_0 \rightarrow 0$. It also differs by an overall sign from the conventional result (4.7) which ignores the back reaction of Hawking radiation.



found in the textbook on classical electromagnetism [25]. According to the Abraham-Lorentz formula, the back-reaction force of the electromagnetic radiation by a point charge is proportional to the 2nd time-derivative of the velocity of the charge. Any solution of a point-charge is then either a runaway solution (accelerating indefinitely to infinite velocity even after all external forces are removed — instability), or it suffers pre-acceleration (acceleration before external forces are applied — violation of causality). The proper way to deal with this issue is of course to keep in mind that, strictly speaking, it is unreasonable to claim a charge to be point-like in a low-energy effective theory. The equation of motion should be solved for a charge with finite size and finite density, and the point charge limit, up to the cut-off scale, should be taken after solving the equation. As long as all charge distributions have a sufficiently smooth profile, these problems can be ignored.

In the light of this analogy, a pseudo thin shell satisfying the inequality (4.20) is a valid thin-shell configuration in the low-energy effective theory, while the ideal thin shell is not.

On the other hand, it is well known that the Abraham-Lorentz formula is still applicable to point charges in perturbative calculations. At the lowest order approximation, a point charge is assumed to move without back reaction. The first order correction to the point-charge trajectory due to back reaction can then be calculated, and it provides a good approximation whenever the radiation is sufficiently weak.

In general, in a low-energy effective theory, one can consider a derivative expansion, which would be truncated at a certain order of the expansion. Assuming that higher derivative terms are less important, the physical result should not be dramatically changed when the order of the truncation is slightly changed. However, higher-derivative terms

always introduce new solutions and new instabilities. An approach to deal with the higher-derivative terms in a low-energy effective theory was suggested by Yang and Feldman [26], which was later extended to a general formulation in Refs. [27]. Following this prescription, one can include the effect of higher-derivative terms order by order without introducing unphysical solutions. In this paper, we adopt this approach to take care of the higher derivatives in the Schwarzian derivative in (2.7).

Notice that, the ideal thin shell without back reaction from Hawking radiation and the pseudo thin shell produces the same formula

$$\frac{da}{du} \simeq -\frac{\kappa \mathcal{N}}{48\pi a^2} \quad (4.25)$$

for Hawking radiation. This is compatible with our analogy with point charges in classical electromagnetism. We will therefore take this formula (4.25) as the lowest order approximation for the Hawking radiation from thin shells. Corrections from higher-order terms in the Schwarzian derivative can then be added iteratively order by order. We will compute the first order correction and check that it is small in our simulations.



Chapter 5

The First Asymptotic States: Slope-1

Shell

Another specific question we would like to answer is whether the smooth configuration studied in Ref. [1] (called the “slope-1” configuration) is the only asymptotic limit for generic initial states. We shall find that there is another asymptotic state.

Yet, in this chapter, we first review the smooth configuration of collapsing matter proposed in Ref. [1]:

$$a(u, r) = \begin{cases} a_0(u) \equiv R_0(u) - \frac{2\sigma}{R_0(u)}, & r > R_0(u), \\ r - \frac{2\sigma}{r}, & R_0(u) > r > \varepsilon, \end{cases} \quad (5.1)$$

where

$$\sigma = \frac{N_0 l_p^2}{48\pi} \quad (5.2)$$

and ε is a small cutoff radius below which the low-energy effective description will no longer be valid. (We assume that ε is much larger than the Planck length.) What happens for $r < \varepsilon$ is irrelevant to the large-scale physics that we are interested in.

The slope of the $a - r$ curve is approximately 1 for this profile, so we will refer to it as a *slope-1 shell*. The slope-1 shell is interesting because it is a solution compatible with the following two assumptions: (1) all particles in the collapsing matter fall at the speed of light, and (2) the decay rate due to Hawking radiation is given by eq.(4.9). We also show in the appendix that slope-1 configurations of arbitrary thickness are unique as asymptotic states under certain assumptions.

The outer radius $R_0(u)$ satisfies eq.(4.5) if it falls at the speed of light. When the shell has sufficiently approached the Schwarzschild radius, $R_0 \simeq a_0(u)$, it can be approximated as

$$R_0(u) = a_0(u) - 2R_0(u) \frac{dR_0(u)}{du} \simeq a_0(u) - 2a_0(u) \frac{da_0}{du} . \quad (5.3)$$

Combining it with eq.(4.9), we see that [1]

$$R_0(u) \simeq a_0(u) + \frac{2\sigma}{a_0(u)} . \quad (5.4)$$

The inverse of this relation is approximated

$$a_0(u) \simeq R_0(u) - \frac{2\sigma}{R_0(u)} . \quad (5.5)$$

For spherically symmetric configurations, we can decompose the collapsing matter into infinitely many infinitesimal collapsing layers labeled by a number α . The total mass enclosed in each shell of radius R_α defines the Schwarzschild radius a_α associated with that shell. (The geometry of the infinitesimal gap between the α -th layer and the $(\alpha + 1)$ -st layer is thus determined by a_α .) Therefore, we can apply the same argument to every

layer below the surface, to claim that eventually

$$R_\alpha(u) \simeq a_\alpha(u) + \frac{2\sigma}{a_\alpha(u)}, \quad (5.6)$$



and hence eq.(5.1) is motivated. This was why the slope-1 configuration was referred to as the “asymptotic black hole” in Ref. [6].

Another quick way to see this is an asymptotic state, as mentioned in Chap.3.1, is by considering again as in the radial trajectory $r(u) = a(u) + \eta$ of a point just outside the Schwarzschild radius, where η is a very small positive constant. Then

$$ds^2 \simeq \left(-\frac{\eta}{a(u)} - 2\frac{da(u)}{du} \right) du^2. \quad (5.7)$$

Assuming $\dot{a}_0(u)$ can be approximated by eq.(4.9), the conclusion is that the collapsing matter can never fall into these regions but at best asymptote to $R_0 \simeq a_0 + \frac{2\sigma}{a_0}$, which is the slope-1 asymptotic state if generalized to every shell.

For this smooth configuration (5.1), eq.(3.21) implies that

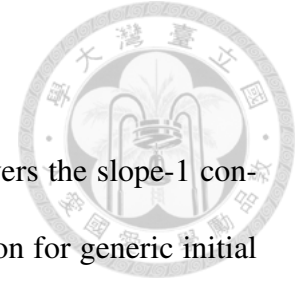
$$\psi_0(u) \simeq -\frac{R_0^2(u)}{4\sigma}, \quad (5.8)$$

so that

$$\dot{\psi}_0(u) \simeq -\frac{R_0(u)\dot{R}_0(u)}{2\sigma} \simeq -\frac{a_0(u)\dot{a}_0(u)}{2\sigma} \simeq \frac{1}{2a_0(u)}. \quad (5.9)$$

Notice that this differs from the conventional result (4.7) for the ideal thin shell by a sign, but the Hawking radiation is the same at the leading order! It is very different from the case of the ideal thin shell when the back reaction of Hawking radiation is taken into consideration.

5.1 Purpose Of Numerical Simulation



It was argued in Ref. [6] that, from the viewpoints of distant observers the slope-1 configuration should be expected to appear as an asymptotic configuration for generic initial states of the collapsing matter.

On the other hand, it was also noted there that, as the surface of the collapsing shell gets very close to the Schwarzschild radius (i.e. when eq.(5.4) is satisfied), everything below a short depth ΔL under the surface is essentially completely frozen. Therefore, it is possible that the collapsing matter demonstrates a different profile under this layer at the surface.

Hence, it is natural to have the following questions. How the collapsing shells with different initial energy distribution approach this limit? How do the profiles of the shells evolve before reaching to this slope-1 limit and whether this limit will always be reached? More precisely, our main question is “what are the asymptotic states of gravitational collapses?” Our task is to study more carefully about the history of the whole collapsing process and how the shells reach the asymptotic limit.

One of the main results of this paper is that we show that even though the slope-1 configuration is indeed an asymptotic state, there exists another asymptotic state, which is simply the pseudo-thin shell described in Chap.4.2.

Before going to discuss the results of numerical simulation, we would like to point out a few setups for numerical simulation.



Chapter 6

Numerical Simulation Setup

In this chapter, we describe the results of our numerical simulation and give an interpretation of the simulation results.

6.1 Each Discrete Shell As Pseudo-thin Shell

In numerical simulations, we shall use discrete collapsing shells as an approximate description of continuous density distribution. For technical issue, the way We label the shells will be the reverse from above, that is we will count the shell by a number $\alpha = 1, 2, \dots, N$ from the inner-most shell ($\alpha = 1$) to the outer-most shell ($\alpha = N$). Each shell has a radius R_α and the total mass M_α enclosed in this shell defines the Schwarzschild radius $a_\alpha = 2GM_\alpha$ associated with this shell. The mass of each shell m_α is $2G(a_\alpha - a_{\alpha-1})$. The space between the α -th shell and the $(\alpha + 1)$ -st shell is then determined by a_α .

The problem is that, as we have demonstrated in Chap.4, the ideal thin shell is unphysical. We should thus identify each discrete shell α not as an ideal thin shell but a pseudo-thin shell. In other words, it evaporates according to the conventional formula for

Hawking radiation (4.9):

$$\frac{da_\alpha}{du_\alpha} \simeq -\frac{N_0 l_p^2}{48\pi a_\alpha^2}, \quad (6.1)$$

where u_α is the outgoing light-cone coordinate for the space between the α -th and the $(\alpha + 1)$ -st shell. As a self-consistency check of this approximation, we shall take eq.(6.1) as the lowest order approximation and calculate the first order correction term through the Schwarzian derivative. In all cases, we find that the first order correction is relatively small.

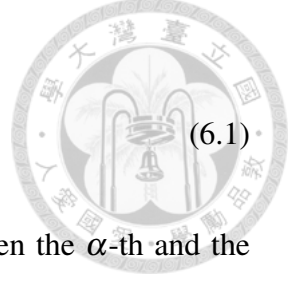
6.2 Removing Higher Derivatives

The discussions on the thin shell in Chap. 4.1 and 4.2 showed that the equation for Hawking radiation (2.7) with the Schwarzian derivative sometimes leads to unphysical results as it is over-sensitive to Planck-scale details. It is also easy to find unphysical behavior such as $da/du > 0$ (negative energy in Hawking radiation) in numerical simulations unless the initial condition is properly chosen. This is not a real surprise as it is well known that higher derivative terms always introduce instabilities into a physical system.

Furthermore, the calculation of the pseudo-thin shell in Chap.4.2 indicated that as a small neighborhood of the shell of thickness ΔL (4.20) is very close to the Schwarzschild radius (so that the separation Δr is of order $\mathcal{O}(\kappa/a)$), the internal region of the collapsing matter below this layer is frozen, and the collapsing matter evaporates according to the conventional rule

$$\frac{da_\alpha(u_\alpha)}{du_\alpha} \simeq \frac{-\sigma}{a_\alpha^2(u_\alpha)} \quad (6.2)$$

for observers immediately outside this layer. Therefore, if we assume that a low-energy configuration cannot have a variation of its profile with a scale shorter than ΔL , the logical



implication is that the conventional formula (6.2) always applies as long as the layer labeled α is very close to its Schwarzschild radius, i.e. $R_\alpha \simeq a_\alpha$.

Our assumption is thus that the conventional formula can be used as a 0-th order approximation for Hawking radiation. In our simulation, we go to the next order by iterating the conventional formula in the exact Schwarzsian derivative. As a self-consistency check, we verify numerically that the correction is small.

More precisely, what we did is the following. The formula for the decay rate of collapsing matter (4.10) applies to every layer of the collapsing shell, with a_0 replaced by a_α , which is twice the Bondi mass enclosed within that layer. Schematically, the Schwarzsian derivative introduces first and second order derivatives as

$$\frac{da_\alpha(u_\alpha)}{du_\alpha} = f(a_\alpha, \dot{a}_\alpha, \ddot{a}_\alpha, R_\alpha), \quad (6.3)$$

where dot means derivative with respect to u_α . In general, there could be first and second derivatives of R_α in the formula, but they can be traded for first and second derivatives of a_α through the evolution equation of R_α

$$\frac{dR_\alpha(u_\alpha)}{du_\alpha} = -\frac{1}{2} \left(1 - \frac{a_\alpha(u_\alpha)}{R_\alpha(u_\alpha)} \right). \quad (6.4)$$

By using this equation repeatedly, the derivatives of R_n can be removed from the expression of f , and therefore, f in (6.3) does not depend on the derivatives of R_n . Thus the decay rate equation (6.3) contains only the derivatives of a_n .

As we explained above, in order to avoid the pathologies introduced by higher derivatives, we will solve the equation by the perturbative method.

We first take the conventional formula (6.2) as the zeroth-order approximation for \dot{a} .

As a result, \ddot{a} is approximate

$$\frac{d^2 a_\alpha(u_\alpha)}{du_\alpha^2} \simeq \frac{-2\sigma^2}{a_\alpha^5(u_\alpha)}, \quad (6.5)$$



so that \dot{a}_α and \ddot{a}_α on the right-hand side of eq.(6.3) can be replaced by functions of a_α , with no time derivatives at all. This way, we get a first order differential equation for a_α . That is, \dot{a}_α is given by a function of a_α and R_α . (It is straightforward to derive this lengthy expression so we will not present it here.) In general, one can do this iteratively to get higher order corrections to obtain a more accurate approximation. We will check that the first order correction is small, and ignore higher-order corrections.

6.3 How To Interpret The Profile

We consider the collapse of matter distribution decomposed as infinitely many spherical shells labeled by a continuous parameter α falling at the speed of light. The radius of each shell α is denoted by $R_\alpha(u)$, and the Bondi mass enclosed within the shell by $m_\alpha(u)$. Corresponding to the mass $m_\alpha(u)$, there is a Schwarzschild radius $a_\alpha(u) = 2m_\alpha(u)$ associated with each shell. Another thing to notice is that in this paper, unless specified, we will always express R_α and a_α with respect to the light-like coordinate $u = u_0$ outside all shells. We assume that there is no horizon in the initial state, that is,

$$R_\alpha(u_{init}) > a_\alpha(u_{init}) \quad (6.6)$$

at the initial time $u = u_{init}$. As time goes on, $R_\alpha(u)$ decreases quickly as the shell with label α collapses at the speed of light. Its associated Schwarzschild radius $a_\alpha(u)$ remains

constant when $R_\alpha(u)$ is sufficiently larger than $a_\alpha(u)$. When $R_\alpha(u)$ gets close to $a_\alpha(u)$, $a_\alpha(u)$ slowly decreases due to Hawking radiation. A horizon emerges when $R_\alpha(u)$ becomes smaller than $a_\alpha(u)$.

While the profile (the $a - r$ graph) of the initial configuration is arbitrary except that it must be a monotonically increasing relation, we shall focus on linear profiles. One can imagine that a generic profile is decomposed into many small segments with each segment approximated by a linear relation between a and r . We shall consider linear $a - r$ relations with various different slopes $\partial a / \partial r$. Once they are understood, it is straightforward to generalize the knowledge to a generic profile by decomposing the profile into many small segments which are approximated by linear relations between a and r .

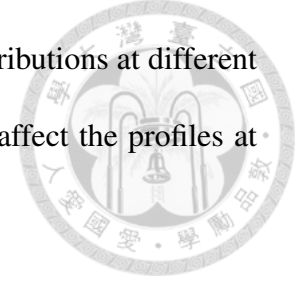
Assuming that all layers α are falling at the speed of light, the radius R_α satisfies the equation

$$\frac{dR_\alpha(u)}{du} = -\frac{1}{2}e^{\psi_\alpha} \frac{R_\alpha - a_\alpha}{R_\alpha}. \quad (6.7)$$

This assumption also ensures that the shells do not cross each other. When the collapsing matter is still far away from its Schwarzschild radius, at large distances where the space-time is nearly flat, the $a - r$ profile remains roughly unchanged as it shifts along the r -axis over time. We shall therefore focus on the initial states in which at least a part of the $a - r$ profile is very close to the $a = r$ line. That is, some of the layers have already approached their Schwarzschild radius $R_\alpha \simeq a_\alpha$ for at least some values of α .

As our main purpose of doing the simulation is to find other asymptotic states, and we already knew that slope-1 configuration is an asymptotic state, we should both consider a small deviation of initial energy density, e.g. $\partial a / \partial r = 1.1$, and also, we would test the much smaller and larger slope cases, e.g. $\partial a / \partial r = 0.1$ and $\partial a / \partial r = \infty$ to cover as large as possible the phase space of initial energy density.

In the following chapter, we will first study the profile of the distributions at different stages. We will check whether different initial energy density will affect the profiles at different stages.



6.4 Massive Core Inside The Collapsing Shells

In order to study the astrophysical black holes, or those which are not very small like the micro black holes, we need to consider a sufficiently large mass. At least the Schwarzschild radius should be much larger than the Planck scale. In order to study such a large mass, a huge number of the layers are necessary. However, the simulations of a lot of layers are computationally expensive. Here, we are interested in the asymptotic states of the collapsing layers, in particular, whether they approach the slope-1 state or evaporate from the outer layers. In order to see this, it is sufficient to study the outer shells. To save computer time in our simulations, we sometimes include a massive core at the center that also evaporates according to the conventional formula (6.1). This way we can efficiently describe a configuration with a large mass, while we focus on the behaviors of the outer shells, and see if they evaporate first. Note that the inner core is essentially frozen because of the strong redshift factor by the outer shells when the outer shells are close to their Schwarzschild radii, so we do not expect the replacement of many inner shells by a massive core to make much difference to the behavior of the outer shells. To verify this assumption, one can compare the dynamics of the outer α layers of a system of $N + \alpha$ layers of collapsing shells, versus the dynamics of α layers in a second system, in which a massive core replaces the N shells of the first system. One can check that the dynamics of the α shells in both systems agree. Furthermore, one can check that the geometry outside all the shells agree with that of a single massive core of the same total mass. Hence the

assumption can be justified by induction.





Chapter 7

Asymptotic States

In this chapter, we will first consider the collapse of shells with different initial energy condition in static Schwarzschild background. This way we get some intuitions about how might the situations change if we turn on the back reaction from Hawking radiation. Then we will study in detail the profiles in time-dependent background.

7.1 a-r Graph In Static Background

For a static Schwarzschild background, assuming every particle in the collapsing shell in free fall, the profile of the collapsing shell should get narrower as it approaches the event horizon, where its profile is completely frozen.

If the initial profile has a slope $\partial a/\partial r$ much smaller than 1, we expect that the inner layers approach their Schwarzschild radii first, and the outer layers to their Schwarzschild radii later. The inner layers do not impose red shift factors to slow down the collapse of outer layers for a distant observer. Therefore, in the end, for distant observers, all the layers are quite close to their Schwarzschild radii, and the profile of the whole collapsing matter is frozen. Such configurations approach states with slopes da/dr approximately

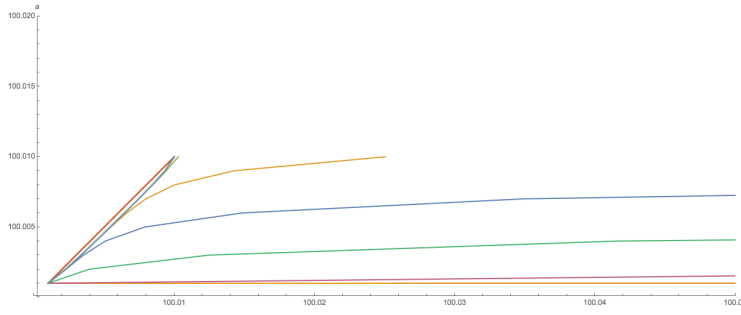
equal to 1, although in detail they are in general different from the slope-1 state described in Chap.5. The attractor states have slope 1 for initial states with sufficiently small slopes da/dr .

If the initial profile has a slope $\partial a/\partial r$ larger than 1, the outer layers approach their Schwarzschild radii earlier, and they impose a large red shift factor on the inner layers from the viewpoint of a distant observer. With the inner layers frozen by the large red-shift factor, the profile of the inner layers remains essentially the same as the initial state. There is no unique asymptotic profile in this case.

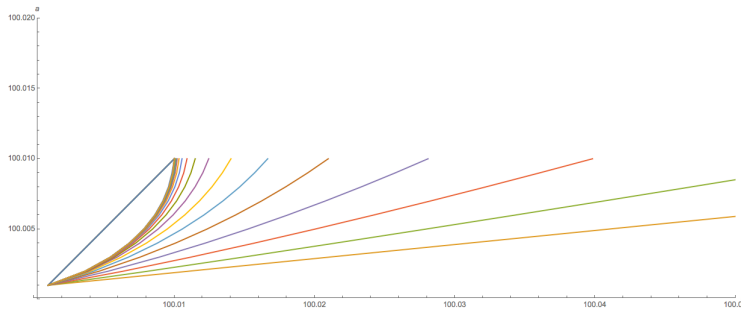
In below, we demonstrate the difference between the profiles using numerical simulation. Please see Fig.7.1. We simulate how the profiles will change with time with different initial energy densities of 0.00001, 0.1, 1.1 and infinity. We put in the diagonal lines which is just $r = a$ for our references.¹

What we wish to understand is how much of this picture is modified by turning on the back reaction of Hawking radiation, so that the Schwarzschild space is time-dependent.

¹ For Fig.7.1a and Fig.7.1b we cut out the right part of the profile for layout of the page.

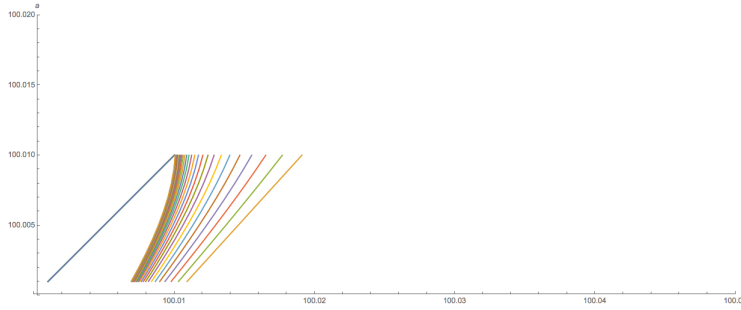


(a) $\partial a/\partial r = 0.00001$

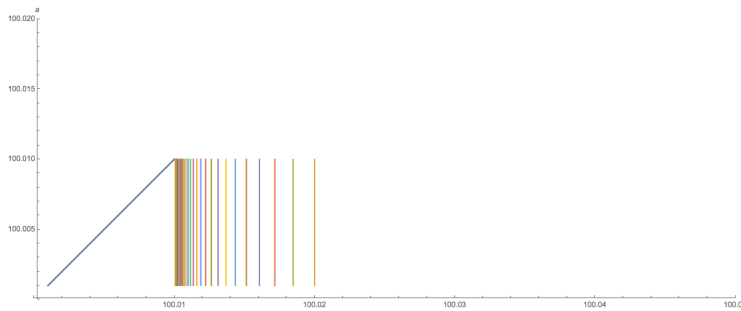


(b) $\partial a/\partial r = 0.1$

it may appear that the shells do not approach slope-1 asymptotic limit. However, for every shell the differences between the position of the shell and its Schwarzschild radius is planck-scale.



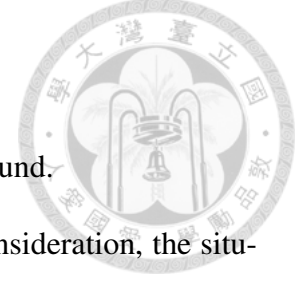
(c) $\partial a/\partial r = 1.1$



(d) $\partial a/\partial r = \infty$

Figure 7.1: a-r graph for $\partial a/\partial r = 0.00001, 1, 1.1, \infty$

7.2 a-r Graph in the KMY Model

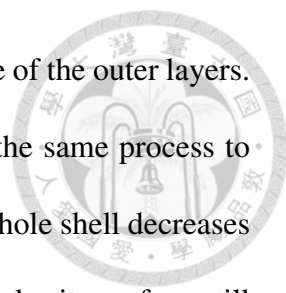


Here we analyze the profiles of the shells in time-dependent background.

When the back reaction of Hawking radiation is taken into consideration, the situation is slightly changed. The geometries between the layers are given by the outgoing Vaidya metric, whose Schwarzschild radii have time dependence and are decreasing due to the effect of Hawking radiation. The profile of the energy distribution is affected by the time dependence of the Schwarzschild radii between the layers.

For a profile with $da/dr \ll 1$, the inner layers would get close to their Schwarzschild radii before the outer layers do theirs, so the inner layers evaporate first. As in the case without the back reaction, the outer layers are never frozen, so they keep falling in, until they also approach their own Schwarzschild radii. Eventually all layers are close to their Schwarzschild radii, and this is the slope-1 configuration (Chap.5). It looks approximately the same as the asymptotic state without the back reaction in Chap.7.1. The effect of the back reaction give no significant modification before the layers approach to the slope-1 configuration. The layers are still moving inward even after it becomes the slope-1 configuration since the Schwarzschild radii are decreasing. However, the profile remains the same.

On the other hand, for an initial state with a large slope $da/dr \gg 1$, the outer layers reach close to their Schwarzschild radii $a(u, r)$ before the inner layers do. The inner layers are frozen by the $1/(r - a)$ contribution of the outer layers to the red-shift factor (3.20), and the outer layers evaporate first. As the outer layers are evaporating, the thickness of the outer layers close to their Schwarzschild radii $a(u, r)$ reduces over time until it is barely thick enough to keep the inner shells frozen. As outer layers evaporate away, inner layers are thawed and start falling close to their Schwarzschild radii. After the evaporation



of the outer layers, the outermost part of the inner layers plays the role of the outer layers. If the profile of the inner layers also has a large slope $da/dr \gg 1$, the same process to the above is repeated by the inner layers. Thus, the thickness of the whole shell decreases over time. Although the inner part of the collapsing matter deep under its surface still has an arbitrary profile depending on the initial condition, the part close to the surface approaches a thin shell. The thin shells can thus be viewed as another class of asymptotic states. The back reaction of Hawking radiation plays an important role in this mechanism. This result is quite different from the case without the back reaction.

In sum, when the radius R_α of a layer α is close to its Schwarzschild radius a_α , the decreasing rate in R_α slows down. If the initial slope is smaller than 1, the innermost layers get close to the curve $a = r$ first, and then, the slope $\partial a/\partial r$ increases over time. If the initial slope is larger than 1, the outermost layers approaches to $a = r$ first. In this case, the inner layers also slows down because of the red shift factor by the outer shells. Therefore, the slope does not decrease. See Figs.7.2–7.5 for the profiles at each moment of the collapse. It should be noted that, for large initial slope of the profile, the effect of the red shift factor appears because the time evolution is measured by using the time coordinate outside all shells. Although the collapse does not slow down for the local observer at the inner layers, it slows down for the observer outside the collapsing matters.

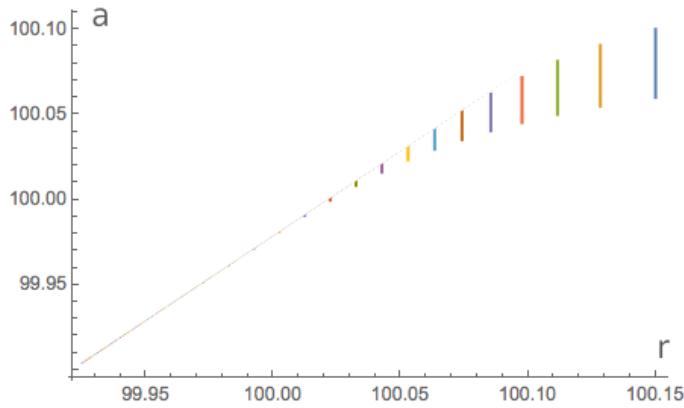


Figure 7.2: $a - r$ graph for $\frac{\partial a}{\partial r} = \infty$
The profile of the collapsing sphere is shown at different instants of u . The initial state with $\frac{\partial a}{\partial r} = \infty$ is the first vertical line from the right. The profile gets shorter as it moves to the left due to evaporation. The slope remains infinite throughout the dynamical process.

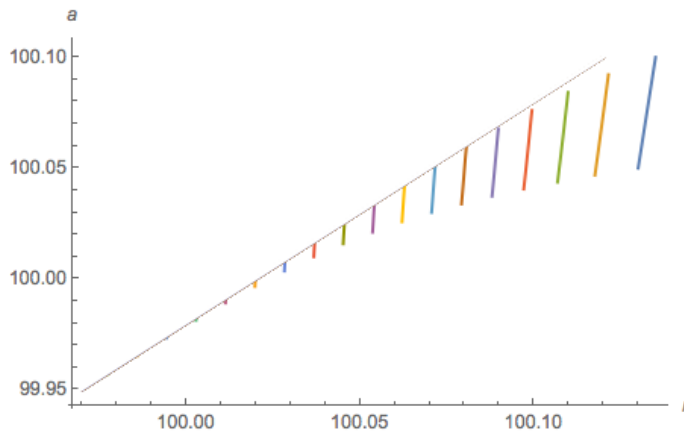


Figure 7.3: $a - r$ graph for $\frac{\partial a}{\partial r} = 10$
The profile of the collapsing sphere is shown at different instants of u . The initial state with $\frac{\partial a}{\partial r} = 10$ is the first vertical line from the right. The profile gets shorter as it moves to the left due to evaporation. The slope approaches infinite in the dynamical process.

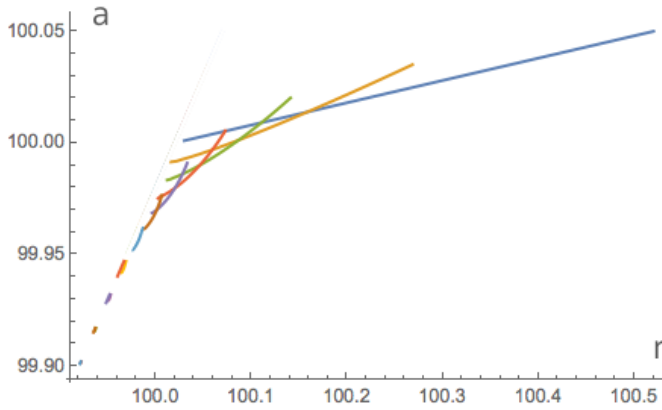


Figure 7.4: $a - r$ graph for $\frac{\partial a}{\partial r} = 0.1$

The profile of the collapsing sphere is shown at different instants of u . The initial state with $\frac{\partial a}{\partial r} = 0.1$ is the first straight line (blue). The profile gets shorter and the slope becomes larger as it moves to the left. Eventually the slope approaches 1.

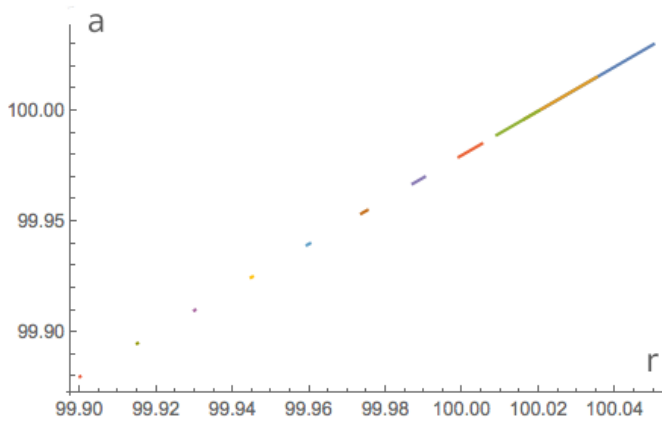


Figure 7.5: $a - r$ graph for $\frac{\partial a}{\partial r} = 1$

The profile of the collapsing sphere is shown at different instants of u . The initial state with $\frac{\partial a}{\partial r} = 1$ is the diagonal line in blue, partially overlapping with the profile at later times. The profile gets shorter and the slope remains approximately equal to 1.

From these simulations, we see that, despite the tendency of increasing the slope $\partial a / \partial r$ over time, once a layer is very close to the $a = r$ line, it can only move diagonally along the $a = r$ line (more precisely, a curve along which $r \simeq a + \frac{2\sigma}{a}$). As a result, for initial configurations with slopes $\partial a / \partial r \ll 1$, the slope only approaches 1 in the end, while configurations with initial slopes $\partial a / \partial r \gg 1$, the slope approaches infinity, which

implies that the collapsing layers approach a thin shell.

To conclude, there are two distinct classes of asymptotic states of black holes. The first class approaches the slope-1 shell, for initial profiles with a small slope. The second class has a slope approaching a pseudo-thin shell for initial profiles with a large slope.

The criterium deciding whether an initial configuration evolves towards one class or another is whether the initial profile da/dr is much smaller than 1 or much larger than 1.

Recall that the density of matter is defined as

$$\frac{dm}{d\text{vol}} = \frac{1}{8\pi G_N r^2} \frac{da}{dr}, \quad (7.1)$$

so the critical volume density ρ_c (around the Schwarzschild radius) corresponding to $da/dr = 1$ is

$$\rho_c \equiv \frac{1}{4\pi r^2} \frac{\partial M}{\partial r} \Big|_{\text{critical}} \simeq \frac{1}{8\pi G_N a^2} = \frac{1}{\kappa a^2}, \quad (7.2)$$

where we have used $a = 2G_N M$.

This corresponds to a volume density of order $\mathcal{O}(1/a^4)$ at a distance of order $\mathcal{O}(a)$ away from the horizon. It is of the same order of magnitude as the Hawking radiation. In fact, ingoing energy of the collapsing matters balances with that of Hawking radiation in the special case of the slope-1 configuration which is studied in [1]. Hence, we expect ingoing energy flux of density higher (lower) than Hawking radiation to resemble the thin shell (slope-1 configuration) as it approaches to the horizon. Even for a black hole as small as a solar mass, its Hawking radiation is much weaker than the current cosmic microwave background radiation. Hence all existing black holes are expected to have a surface layer resembling the thin shell configuration. That is, the slope da/dr is very large at the surface of the black hole.

7.3 Details Of The Profiles

In the KMY model, it was found [1] that, for the ideal slop-1 shells, the collapsing shells are getting inward as they lose the energy by Hawking radiation, and completely evaporate when they mostly reached to the center of the star. It is also argued [4] that the evaporation of the collapsing shells, in most cases, happens in the same fashion as peeling an onion — layer by layer from the outside. The reason is that the inner shells are frozen due to the huge red-shift factor.

Here we would like to ask in general, when would the evaporation starts from the layers on the outside or the inside. In order to see this, we calculate the time evolution of the Schwarzschild radii for each shell, as functions of u . We find that the evaporation process is a competition between the suppression due to a large red-shift factor and the enhancement of evaporation due to the short separation of a layer from its Schwarzschild radius a . The details are described in the following.

7.4 Small Slope

For a collapsing profile with a very small slope ($\partial a/\partial r \ll 1$), the innermost shell approaches its Schwarzschild radius before other shells and starts to evaporate first. As more and more layers approach their Schwarzschild radii, a layer that is already close to its Schwarzschild radii will stay locked at a separation $R_\alpha - a_\alpha \simeq 2\sigma/a_\alpha$ until it is evaporated.

As the outer layers are close to their Schwarzschild radii, the red-shift factor becomes large for the remaining inner layers, so that the radiation of the remaining inner layers is suppressed. The outer layers are then evaporated before them.



Therefore, for a collapsing profile with a tiny slope, its evaporation can be very roughly decomposed into two stages. In the first stage, the inner layers evaporate first, and the outer layers are still far from their Schwarzschild radii. In the 2nd stage², the outer layers get close to their Schwarzschild radii and start to evaporate, and the inner layers surviving the first stage are frozen until the outer layers are evaporated. The configuration of the collapsing matter is now in agreement with the slope-1 shell.

This process is shown in Fig.7.6. The plot consists of many lines of the Schwarzschild radii for each shell. A layer completely evaporates when the line crosses to the inner line — its Schwarzschild radius becomes the same to that of the inner layer. In comparison, the process for $\partial a/\partial r \simeq 1$ is shown in Fig.7.7, for which the outer layers are evaporated first, resembling the late stage of Fig.7.6.

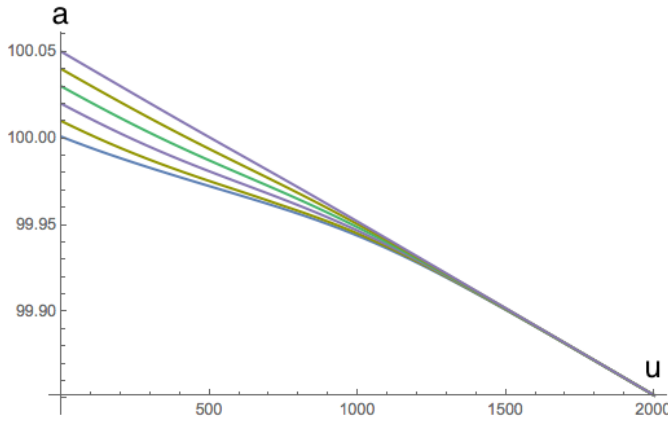


Figure 7.6: $a(u)$ for $da/dr = 0.1$

The values a_α for all layers are shown as functions of time u . The values of a_α do not start at 0 because there is a massive core at the center. The inner-most layers evaporate first, so in the diagram they merge with other layers initially on top of them. At larger u , the outer-most layers evaporate and appear to merge with other layers initially under them.

² This is the stage of onion peeling described in the KMY model

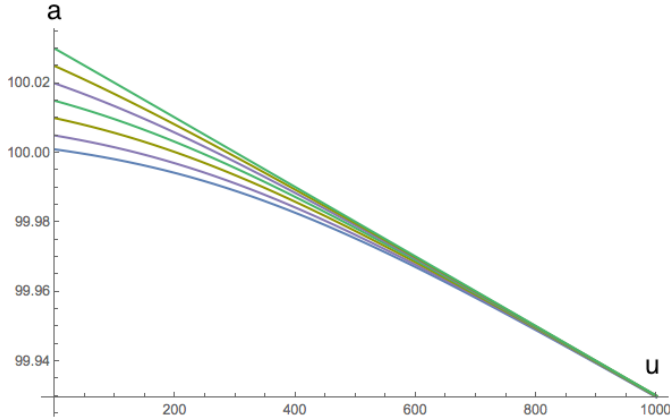


Figure 7.7: $a(u)$ for $da/dr = 1$

The values a_α for all layers are shown as functions of time u . The values of a_α do not start at 0 because there is a massive core at the center. The outer-most layers evaporate first so they appear to merge with other layers initially under them.

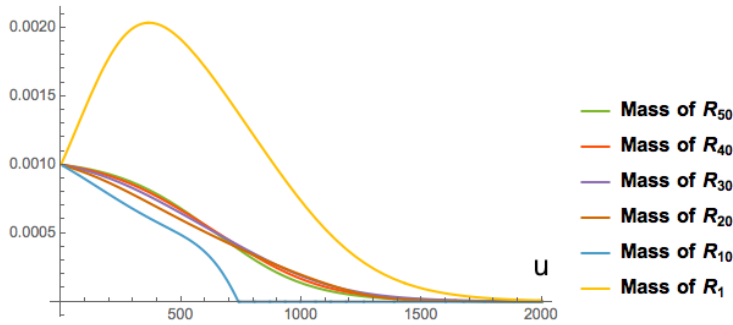


Figure 7.8: $m(u)$ for $\partial a/\partial r = 0.1$

The masses of some of the layers are shown as functions of time u . It is clear that, generically, inner layers evaporate faster in the beginning, while outer layers evaporate faster at a later time. There is roughly a point of intersection of the curves when they have evaporated the same percentage of their masses. The mass of the first layer R_1 outside the massive core appears to be anomalous as it initially increases with time. This is because the outgoing energy due to the evaporation of the massive core is temporarily counted as its energy. This is merely an artifact of our choice of the configuration. By studying the behaviors of the outer part of the distribution, we can still get a very clear picture of how the shells evolve.

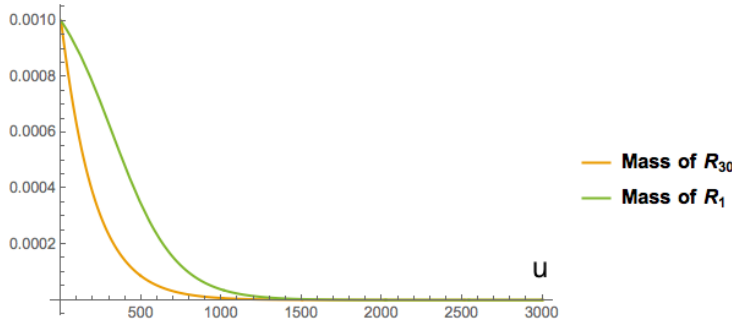


Figure 7.9: $m(u)$ for $\partial a / \partial r = 1$

The masses of some of the layers are shown as functions of time u . The situation is simple in this case: outer layers evaporate faster than inner layers at all times.

7.5 Large Slope

For a collapsing profile with a large slope ($\partial a / \partial r \gg 1$), the outer layers get close to their Schwarzschild radii earlier than the inner ones. Hence the inner layers are frozen until outer layers are evaporated.

Whenever the outer layers are very close to its Schwarzschild radius, the inner layers are frozen by the large red-shift factor and the radiation of the inner layers can be ignored regardless of whether the inner layers are close to their own Schwarzschild radii. Therefore, for a collapsing ball with an outer surface that has been evaporating for a long time, it is always evaporating from the outer layers. An exception would be the stationary solution which is studied in [1]. In this case, the inner layers are also very close to their Schwarzschild radii and the evaporation proceeds simultaneously. On the other hand, even in this case, although the inner layers completely evaporates first, the process is extremely slow because of the very large redshift factor, and the Hawking radiation mostly comes from the outer layers.

The inner layers stay frozen until the outer layers are evaporated. For an outer layer as close to the Schwarzschild radius as $R - a \sim \mathcal{O}(\sigma/a)$, the red-shift factor for the layer

at a separation ΔR under the outer surface is of order $e^{-R_0 \Delta R / 2\sigma}$. Roughly speaking, it is natural to think of a layer of matter to have the thickness of a Planck length and a layer is evaporated before the next layer starts to evaporate.

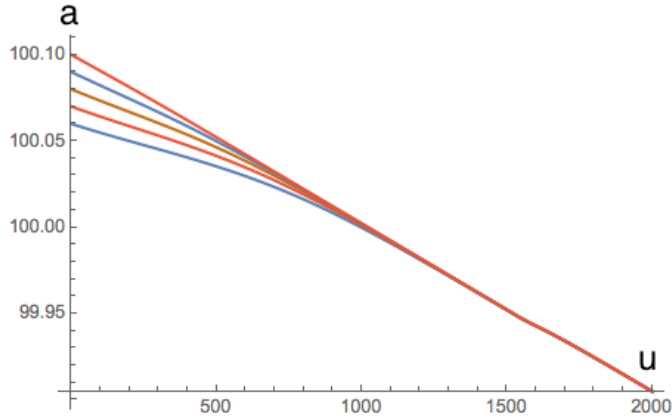
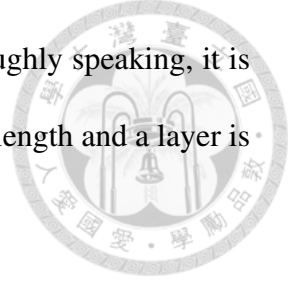


Figure 7.10: $a(u)$ for $\partial a / \partial r = \infty$

The values a_α for all layers are shown as functions of time u . The values of a_α do not start at 0 because there is a massive core at the center. The outer-most layers evaporate first, so in the diagram they appear to merge with other layers initially below them.

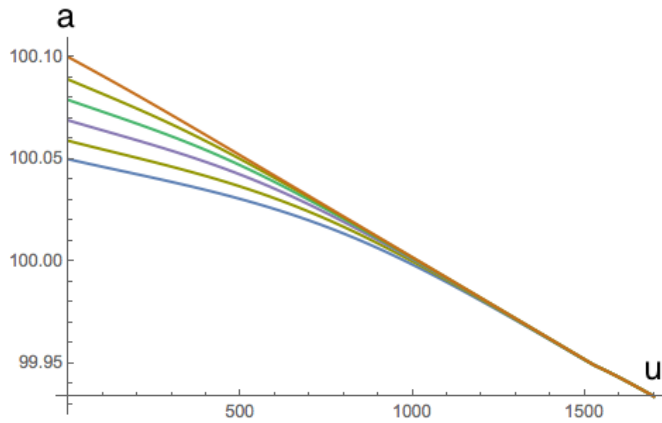


Figure 7.11: $a(u)$ for $\partial a / \partial r = 10$

This diagram is essentially the same as Fig.7.10.

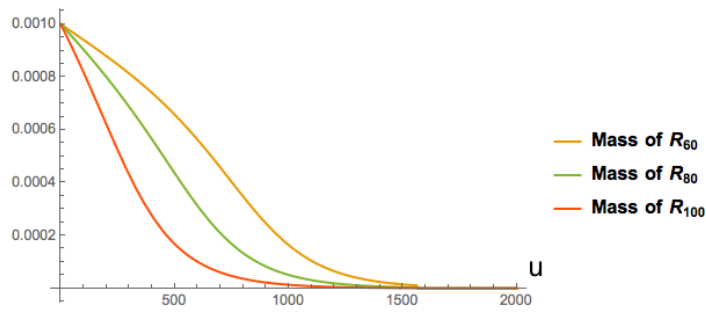


Figure 7.12: $m(u)$ for $\partial a / \partial r = \infty$
The masses of some of the layers are shown as functions of time u . Generically, outer layers evaporate faster.

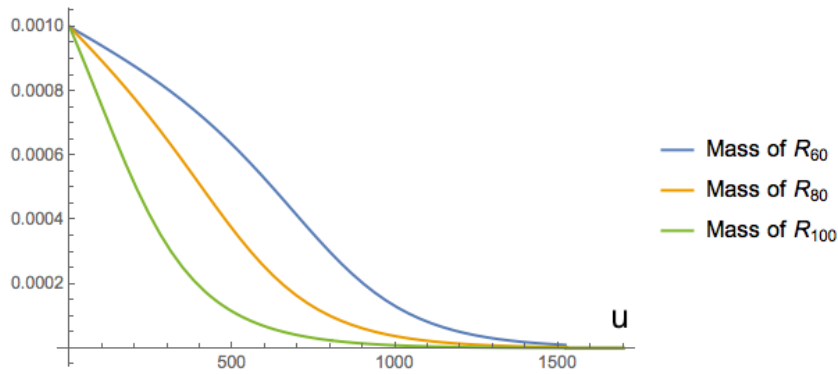


Figure 7.13: $m(u)$ for $\partial a / \partial r = 10$
This diagram is essentially the same as Fig.7.12.

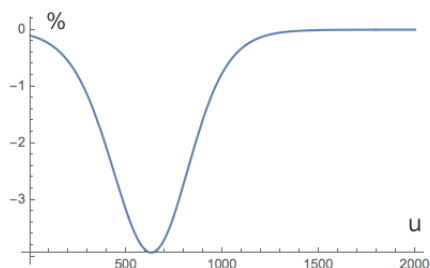


Chapter 8

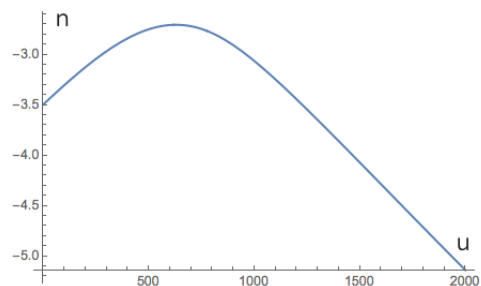
Stability Of The Decaying Rate

In Chap.6.4 we mention that as a consistency check for using the perturbation method to calculate \dot{a} and also for putting a massive core inside the shells, we should check whether \dot{a} can be approximated by the conventional formula. We find that there is some instability initially for \dot{a} when using the Schwarzian derivative. For both $\frac{da}{dr}$ equal to 0.1 and 1, the first order correction to the 0-th order Hawking radiation is relatively small. We analyzed this deviation in three different ways: (1) the percentage of correction with respect to the 0-th order amplitude: $\Delta\left(\frac{da}{du}\right)/\frac{da^{(0)}}{du}$, (2) how the correction $\Delta\left(\frac{da}{du}\right)$ scales with a during the collapsing process, and (3) If we use the formula $\frac{da}{du} = -C(u)\sigma/a^2$ to model the Hawking radiation, how is the coefficient $C(u)$ changing with time. In all analyses we find the first order correction to Hawking radiation sufficiently small to justify our perturbative interpretation of the Schwarzian derivative. See Fig.8.1 for $\frac{da}{dr} = 0.1$ and Fig.8.2 for $\frac{da}{dr} = 1$.

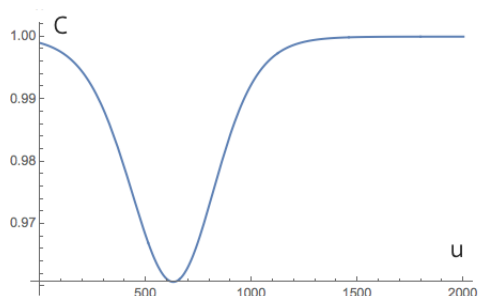
We also check the validity of the perturbation, again. For both $\frac{da}{dr} = \infty$ and $\frac{da}{dr} = 10$, the first order correction to the 0-th order Hawking radiation is also very small, as the case of small slopes.



(a) The first order correction $\Delta\left(\frac{da}{du}\right)$ as percentage of the 0-th order expression of $\frac{da}{du}$.

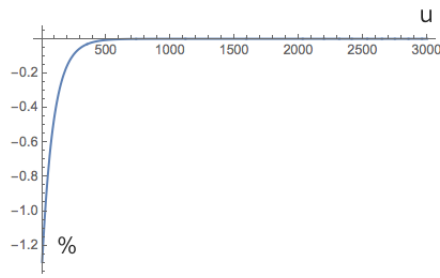


(b) Modelling the dependence of the first order correction $\Delta\left(\frac{da}{du}\right)$ by power law $\Delta\left(\frac{da}{du}\right) = Aa^n$ for some constant A .

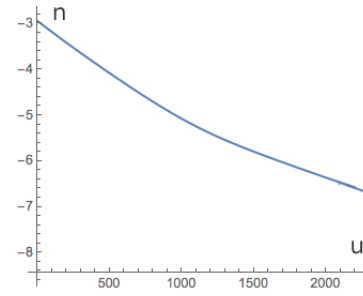


(c) Modelling the first order correction by the coefficient C in $\Delta\left(\frac{da}{du}\right) = \frac{(1-C)\sigma}{a^2}$.

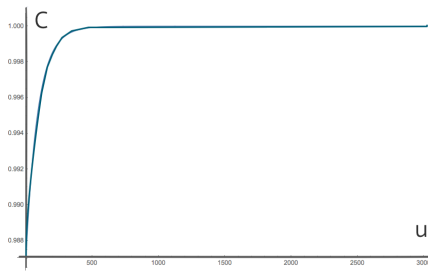
Figure 8.1: The first order correction in Hawking radiation for $\frac{da}{dr} = 0.1$



(a) The first order correction $\Delta\left(\frac{da}{du}\right)$ as percentage of the 0-th order expression of $\frac{da}{du}$.

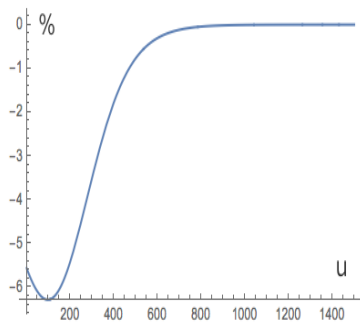


(b) Modelling the dependence of the first order correction $\Delta\left(\frac{da}{du}\right)$ by power law $\Delta\left(\frac{da}{du}\right) = Aa^n$ for some constant A .

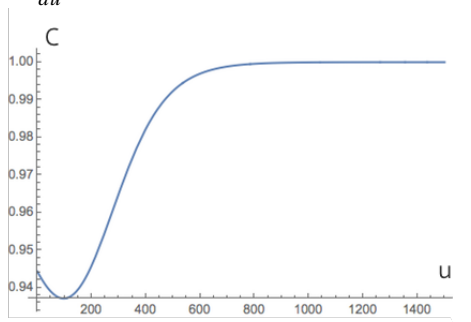


(c) Modelling the first order correction by the coefficient C in $\Delta\left(\frac{da}{du}\right) = \frac{(1-C)\sigma}{a^2}$.

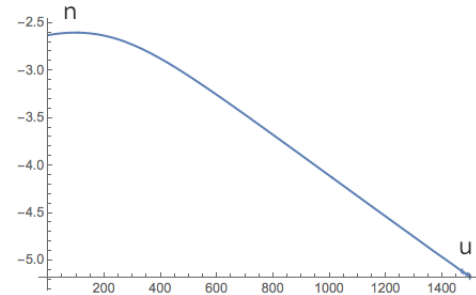
Figure 8.2: The first order correction in Hawking radiation for $\frac{da}{dr} = 1$.



(a) The first order correction $\Delta\left(\frac{da}{du}\right)$ as percentage of the 0-th order expression of $\frac{da}{du}$.

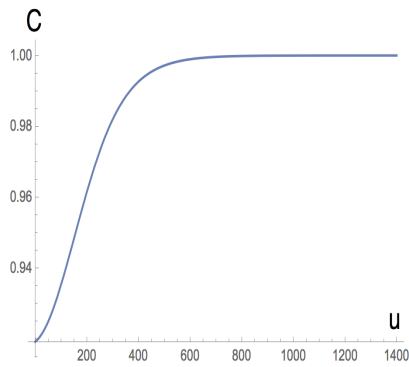


(c) Modelling the first order correction by the coefficient C in $\Delta\left(\frac{da}{du}\right) = \frac{(1-C)\sigma}{a^2}$.

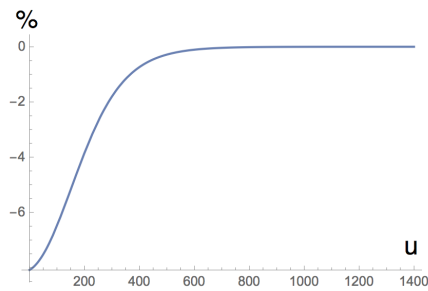


(b) Modelling the dependence of the first order correction $\Delta\left(\frac{da}{du}\right)$ by power law $\Delta\left(\frac{da}{du}\right) = Aa^n$ for some constant A .

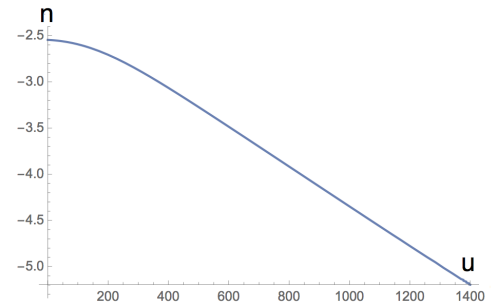
Figure 8.3: The first order correction in Hawking radiation for $\frac{da}{dr} = \infty$



(a) The first order correction $\Delta\left(\frac{da}{du}\right)$ as percentage of the 0-th order expression of $\frac{da}{du}$.



(c) Modelling the first order correction by the coefficient C in $\Delta\left(\frac{da}{du}\right) = \frac{(1-C)\sigma}{a^2}$.



(b) Modelling the dependence of the first order correction $\Delta\left(\frac{da}{du}\right)$ by power law $\Delta\left(\frac{da}{du}\right) = Aa^n$ for some constant A .

Figure 8.4: The first order correction in Hawking radiation for $\frac{da}{dr} = 10$



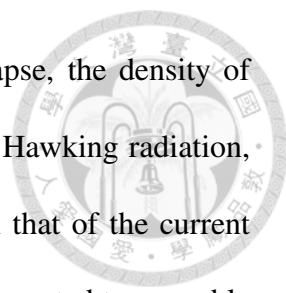
Chapter 9

Discussion and Conclusion

In this work, we studied the dynamical process of collapsing spheres in the KMY model, in which the Schwarzschild radii are time-dependent due to the back reaction of Hawking radiation.

First of all, we demonstrate the unphysicalness of using an ideal thin shell to describe black hole physics. While an ideal thin shell does not completely evaporate in the KMY model, a pseudo thin shell does. The origin of this over-sensitivity on short-distance features is the higher derivatives needed to determine Hawking radiation. By properly treating the higher derivative terms, the discrepancy between the ideal thin shell and pseudo thin shell disappears. All smooth configurations evaporate completely within finite time.

Secondly, we showed that there are two classes of asymptotic states in the KMY model. We find that besides the slope-1 asymptotic state, there exist another one which is called the *pseudo-thin shell*. These two types are distinguished by the critical energy density ρ_c (7.2). When the initial energy density is higher than the critical energy density, the collapsing shell approaches the pseudo-thin shell state. On the other hand, if the initial energy density is lower than ρ_c , the collapsing shell approaches the slope-1 shell state.



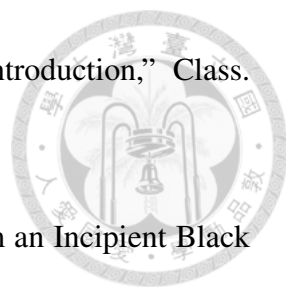
In order to have the critical density after the gravitational collapse, the density of the matter when it starts to collapse is of the same order as that of Hawking radiation, which is, for a large range of black-hole masses, much smaller than that of the current CMB. Therefore, the outer layers of black holes at present time are expected to resemble a (pseudo) thin shell configuration.


Notice that despite the apparent difference between the profiles of the slope-1 shell and the pseudo-thin shell, both configurations appear to be very similar from the viewpoint of a distant observer. The reason is that the matter at a Planck length under the surface of the shell is essentially frozen and unobservable [6]. It will be interesting to investigate how these asymptotic states can be distinguished by certain high-precision observations.



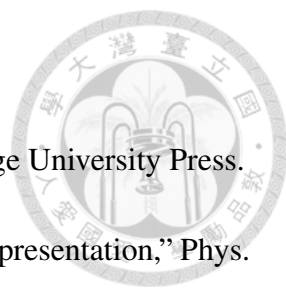
Bibliography

- [1] H. Kawai, Y. Matsuo and Y. Yokokura, “A Self-consistent Model of the Black Hole Evaporation,” *Int. J. Mod. Phys. A* **28**, 1350050 (2013) [arXiv:1302.4733 [hep-th]].
- [2] H. Kawai and Y. Yokokura, “Phenomenological Description of the Interior of the Schwarzschild Black Hole,” arXiv:1409.5784 [hep-th].
- [3] P. M. Ho, “Comment on Self-Consistent Model of Black Hole Formation and Evaporation,” arXiv:1505.02468 [hep-th].
- [4] H. Kawai and Y. Yokokura, “Interior of Black Holes and Information Recovery,” arXiv:1509.08472 [hep-th].
- [5] P. M. Ho, “The Absence of Horizon in Black-Hole Formation,” arXiv:1510.07157 [hep-th].
- [6] P. M. Ho, “Asymptotic Black Holes,” *Class. Quant. Grav.* **34**, no. 8, 085006 (2017) doi:10.1088/1361-6382/aa641e [arXiv:1609.05775 [hep-th]].
- [7] P. H. Lambert, “Introduction to Black Hole Evaporation,” *PoS Modave* **2013**, 001 (2013) doi:10.22323/1.201.0001 [arXiv:1310.8312 [gr-qc]].
- [8] J. G. Russo, L. Susskind and L. Thorlacius, “The Endpoint of Hawking radiation,” *Phys. Rev. D* **46**, 3444 (1992) doi:10.1103/PhysRevD.46.3444 [hep-th/9206070].

- 
- [9] S. D. Mathur, “The Information paradox: A Pedagogical introduction,” *Class. Quant. Grav.* **26**, 224001 (2009) [arXiv:0909.1038 [hep-th]].
- [10] U. H. Gerlach, “The Mechanism of Black Body Radiation from an Incipient Black Hole,” *Phys. Rev. D* **14**, 1479 (1976). doi:10.1103/PhysRevD.14.1479
- [11] C. R. Stephens, G. ’t Hooft and B. F. Whiting, “Black hole evaporation without information loss,” *Class. Quant. Grav.* **11**, 621 (1994) doi:10.1088/0264-9381/11/3/014 [gr-qc/9310006].
- [12] G. ’t Hooft, “The Scattering matrix approach for the quantum black hole: An Overview,” *Int. J. Mod. Phys. A* **11**, 4623 (1996) doi:10.1142/S0217751X96002145 [gr-qc/9607022].
- [13] O. Lunin and S. D. Mathur, “AdS / CFT duality and the black hole information paradox,” *Nucl. Phys. B* **623**, 342 (2002) [hep-th/0109154]. O. Lunin and S. D. Mathur, “Statistical interpretation of Bekenstein entropy for systems with a stretched horizon,” *Phys. Rev. Lett.* **88**, 211303 (2002) [hep-th/0202072].
- [14] T. Vachaspati, D. Stojkovic and L. M. Krauss, “Observation of incipient black holes and the information loss problem,” *Phys. Rev. D* **76**, 024005 (2007) doi:10.1103/PhysRevD.76.024005 [gr-qc/0609024].
- [15] C. Barcelo, S. Liberati, S. Sonego and M. Visser, “Fate of gravitational collapse in semiclassical gravity,” *Phys. Rev. D* **77**, 044032 (2008) doi:10.1103/PhysRevD.77.044032 [arXiv:0712.1130 [gr-qc]].
- [16] T. Kruger, M. Neubert and C. Wetterich, “Cosmon Lumps and Horizonless Black Holes,” *Phys. Lett. B* **663**, 21 (2008) doi:10.1016/j.physletb.2008.03.051 [arXiv:0802.4399 [astro-ph]].

- 
- [17] S. Yi, “Black hole: Never forms, or never evaporates,” JCAP **1101**, 031 (2011) [arXiv:1102.2609 [physics.gen-ph]]
- [18] F. Fayos and R. Torres, “A quantum improvement to the gravitational collapse of radiating stars,” Class. Quant. Grav. **28**, 105004 (2011). doi:10.1088/0264-9381/28/10/105004
- [19] L. Mersini-Houghton, “Backreaction of Hawking Radiation on a Gravitationally Collapsing Star I: Black Holes?,” PLB30496 Phys Lett B, 16 September 2014 [arXiv:1406.1525 [hep-th]]. L. Mersini-Houghton and H. P. Pfeiffer, “Back-reaction of the Hawking radiation flux on a gravitationally collapsing star II: Fireworks instead of firewalls,” arXiv:1409.1837 [hep-th].
- [20] A. Saini and D. Stojkovic, “Radiation from a collapsing object is manifestly unitary,” Phys. Rev. Lett. **114**, no. 11, 111301 (2015) [arXiv:1503.01487 [gr-qc]].
- [21] V. Baccetti, R. B. Mann and D. R. Terno, “Role of evaporation in gravitational collapse,” Class. Quant. Grav. **35**, no. 18, 185005 (2018) doi:10.1088/1361-6382/aad70e [arXiv:1610.07839 [gr-qc]].
- [22] V. Baccetti, R. B. Mann and D. R. Terno, “Do event horizons exist?,” Int. J. Mod. Phys. D **26**, no. 12, 1743008 (2017) doi:10.1142/S0218271817430088, 10.1142/S0218271817170088 [arXiv:1706.01180 [gr-qc]].
- [23] P. C. W. Davies and S. A. Fulling, “Radiation from a moving mirror in two-dimensional space-time conformal anomaly,” Proc. Roy. Soc. Lond. A **348**, 393 (1976).
- [24] P. C. W. Davies, S. A. Fulling and W. G. Unruh, “Energy Momentum Tensor Near an Evaporating Black Hole,” Phys. Rev. D **13**, 2720 (1976).

doi:10.1103/PhysRevD.13.2720

- 
- [25] David J. Griffiths, “Introduction to Electrodynamics”, Cambridge University Press.
- [26] C. N. Yang and D. Feldman, “The S Matrix in the Heisenberg Representation,” *Phys. Rev.* **79**, 972 (1950). doi:10.1103/PhysRev.79.972
- [27] T. C. Cheng, P. M. Ho and M. C. Yeh, “Perturbative approach to higher derivative and nonlocal theories,” *Nucl. Phys. B* **625**, 151 (2002) doi:10.1016/S0550-3213(02)00020-2 [hep-th/0111160]. T. C. Cheng, P. M. Ho and M. C. Yeh, “Perturbative approach to higher derivative theories with fermions,” *Phys. Rev. D* **66**, 085015 (2002) doi:10.1103/PhysRevD.66.085015 [hep-th/0206077].
- [28] M. W. Choptuik, “Universality and scaling in gravitational collapse of a massless scalar field,” *Phys. Rev. Lett.* **70**, 9 (1993). doi:10.1103/PhysRevLett.70.9 C. Gundlach, “Critical phenomena in gravitational collapse,” *Adv. Theor. Math. Phys.* **2**, 1 (1998) [gr-qc/9712084]. For a review, see: C. Gundlach and J. M. Martin-Garcia, “Critical phenomena in gravitational collapse,” *Living Rev. Rel.* **10**, 5 (2007) doi:10.12942/lrr-2007-5 [arXiv:0711.4620 [gr-qc]].



Appendix: Derivative Expansion of Thin Shells

Here we verify that, under certain assumptions about the asymptotic limit, the slope-1 shells of arbitrary thickness (including the pseudo thin shell) are the only lowest-order solutions in the derivative expansion of the formulas of Hawking radiation. The equations of Hawking radiation in the KMY model are eqs.(3.22), (3.23), (4.5), and (4.10). The lowest-order approximation of eq.(3.23) is ¹

$$\{u, U\} \simeq \frac{1}{3} \psi_0^2. \quad (9.1)$$

First of all, it should be clear that the Hawking radiation is dominated by the contributions of those layers in the collapsing shell that are very close to their Schwarzschild radii. It is also obvious that, in terms of the coordinate u suitable for a distant observer, these layers spend a very long time approaching their Schwarzschild radii. The assumption we make is that the distribution of these layers eventually approach a certain universal asymptotic profile

$$R(a) - a \simeq f(a) \quad (9.2)$$

¹ There is in fact an ambiguity in the derivative expansion depending on which variable (ψ_0 vs. dU/du) is used.

for a certain given function $f(a)$ that depends only on a and other physical constants. As the only relevant constant parameter in this model is σ (or $\kappa\mathcal{N}$), $f(a)$ can always be rewritten as $ag(\sigma/a^2)$ for a certain function g . Since σ/a^2 is an extremely tiny number, it is dominated by the leading order term in its power expansion in σ/a^2 . Therefore, we assume that

$$R(a) - a \simeq \frac{C}{a^n} \quad (9.3)$$

at the leading order in the (σ/a^2) -expansion for a constant C and a number n . (This assumption excludes ideal thin shells.) A generic consequence of this is that

$$\dot{R}(a) - \dot{a} \simeq 0 \quad (9.4)$$

at the leading order. Taking u -derivatives on this equation and using eq.(4.5), we find

$$\dot{a}_0 \simeq \dot{R}_0 \simeq -\frac{R_0 - a_0}{2R_0} \simeq -\frac{C}{2a_0^{n+1}}. \quad (9.5)$$

According to eq.(3.22),

$$\psi_0 \simeq -\frac{a_0^{n+1}}{(n+1)C}. \quad (9.6)$$

Then eqs.(4.10) and (9.1) imply

$$\dot{a}_0 \simeq -\frac{\kappa\mathcal{N}}{12\pi} \psi_0^2 \simeq -\frac{\kappa\mathcal{N}}{12\pi} \frac{a_0^{2n}}{C^2} \dot{a}_0^2, \quad (9.7)$$

from which we find

$$\dot{a}_0 \simeq -\frac{12\pi}{\kappa\mathcal{N}} \frac{C^2}{a_0^{2n}}. \quad (9.8)$$

The agreement between eqs.(9.5) and (9.8) demands that

$$n = 1,$$

$$C = \frac{\kappa \mathcal{N}}{24\pi}. \quad (9.10)$$



Therefore the asymptotic profile (9.3) is precisely the slope-1 configuration (without restriction on its thickness so pseudo thin shells are included). For the self consistency of this result, one can check that the higher order terms ignored in eq.(9.1) are indeed much smaller than the lower order terms.